First search for nontensorial gravitational waves from known pulsars

The LIGO Scientific Collaboration and the Virgo Collaboration
(Dated: September 28, 2017)

We present results from the first directed search for nontensorial gravitational waves. While general relativity allows for tensorial (plus and cross) modes only, a generic metric theory may, in principle, predict waves with up to six different polarizations. This analysis is sensitive to continuous signals of scalar, vector or tensor polarizations, and does not rely on any specific theory of gravity. After searching data from the first observation run of the advanced LIGO detectors for signals at twice the rotational frequency of 200 known pulsars, we find no evidence of gravitational waves of any polarization. We report the first upper limits for scalar and vector strains, finding values comparable in magnitude to previously-published limits for tensor strain. Our results may be translated into constraints on specific alternative theories of gravity.

arXiv:1709.09203v1 [gr-qc] 26 Sep 2017

Introduction. The first gravitational waves (GWs) detected by the Advanced Laser Interferometer Gravitational-wave Observatory (aLIGO) have already been used to place some of the most stringent constraints on deviations from the general theory of relativity (GR) in the highly-dynamical and strong-field regimes of gravity [1–4]. However, it has not been possible to unambiguously confirm GR's prediction that the associated metric perturbations are of a tensor nature (helicity ± 2), rather than vector (helicity ± 1), or scalar (helicity 0) [5]. This is unfortunate, since the presence of nontensorial modes is a key prediction of many extensions to GR [6–10]. Most importantly, the detection of a scalar or vector component, no matter how small, would automatically falsify Einstein's theory [8, 9].

In order to experimentally determine whether gravitational waves are tensorial or not in a model-independent way, one needs a local measurement of the signal's polarization content that breaks the degeneracies between the five distinguishable modes supported by a generic metric theory of gravity [6, 7]. For transient waves like those detected so far, this cannot be achieved with LIGO's two detectors, as at least five noncooriented differential-arm antennas would be required to break *all* such degeneracies [9, 11]. Constraints on the magnitude of non-GR polarizations inferred from indirect measurements, like that of the rate of orbital decay of binary pulsars, are only meaningful in the context of specific theories (see e.g. [12, 13], or [14, 15] for reviews).

Theory-independent polarization measurements could instead be carried out with current detectors in the presence of signals sufficiently long to probe the detector antenna patterns, which are themselves polarization-sensitive [16–19]. Such is the case, for instance, for the continuous, almost-monochromatic waves expected from spinning neutron stars with an asymmetric moment of inertia [20]. Known galactic pulsars are one of the main candidates for searches for such signals in data from ground-based detectors, and analyses targeting them have already achieved sensitivities that are comparable to, or even surpass, their canonical spin-down limit (i.e. the strain that would be produced if the observed slowdown in the pulsar's rotation was completely due to gravitational radiation) [21].

However, all previous targeted searches have been, by design, restricted to tensorial gravitational polarizations *only*. This leaves open the possibility that, due to a departure from GR, the neutron stars targeted in previous searches may indeed be emitting strong continuous waves with nontensorial content, in spite of the null results of standard searches.

In this paper, we present results from a search for continuous gravitational waves in aLIGO data that makes no assumptions about how the gravitational field transforms under spatial rotations, and is thus sensitive to any of the six polarizations allowed by a generic metric theory of gravity. We targeted 200 known pulsars using data from aLIGO's first observation run (O1), and assuming GW emission at twice the rotational frequency of the source.

Our data provide no evidence for the emission of gravitational signals of tensorial or nontensorial polarization from any of the pulsars targeted. For sources in the most sensitive band of our detectors, we constrain the strain of the scalar and vector modes to be below 1.5×10^{-26} at 95% credibility. These are the first direct upper limits for scalar and vector strain ever published, and may be used to constrain beyond-GR theories of gravity.

Analysis. We search aLIGO O1 data from the Hanford (H1) and Livingston (L1) detectors for continuous waves of any polarization (tensor, scalar or vector) by applying the Bayesian time-domain method of [22], generalized to non-GR modes as described in [17] and summarized below. Our analysis follows closely that of [21], and uses the exact same interferometric data.

Calibrated detector data are heterodyned and filtered using the timing solutions for each pulsar obtained from electromagnetic observations. The maximum calibration uncertainties estimated over the whole run give a limit on the combined H1 and L1 amplitude uncertainties of 14%—this is the conservative level of uncertainty on the strain upper limits [21, 23].

The data streams start on 2015 Sep 11 at 01:25:03 UTC for H1 and 18:29:03 UTC for L1, and finish on 2016 Jan 19 at 17:07:59 UTC at both sites. The pulsar

timing solutions used are also the same as in [21] and were obtained from the 42-ft telescope and Lovell telescope at Jodrell Bank (UK), the 26-m telescope at Hartebeesthoek (South Africa), the Parkes radio telescope (Australia), the Nancay Decimetric Radio Telescope (France), the Arecibo Observatory (Puerto Rico) and the Fermi Large Area Telescope (LAT).

As described in detail in [17], we construct a Bayesian hypothesis that captures signals of any polarization content (our *any-signal* hypothesis, $\mathcal{H}_{\rm S}$) by combining the sub-hypotheses corresponding to the signal being composed of tensor, vector, scalar modes, or any combination thereof. Each of these sub-hypotheses corresponds to a different signal model; in particular, the least restrictive template includes contributions from all polarizations and can be written as:

$$h(t) = \sum_p F_p(t;\alpha,\delta,\psi) h_p(t), \tag{1}$$

where the sum is over the five independent polarizations: plus (+), cross (×), vector-x (x), vector-y (y) and scalar (s) [7]. The two scalar modes, breathing and longitudinal, are degenerate for networks of quadrupolar antennas [9], so we do not make a distinction between them.

Each term in Eq. (1) is the product of an antenna pattern function F_p and an intrinsic strain function h_p. We define the different polarizations in a wave-frame such that the z-axis points in the direction of propagation, x lies in the plane of the sky along the line of nodes (here defined to be the intersection of the equatorial plane of the source with the plane of the sky), and y completes the right-handed system, such that the polarization angle ψ is the angle between the y-axis and the projection of the celestial North onto the plane of the sky (see e.g. [24]). We can thus write the F_p's as implicit functions of the source's right ascension α, declination δ and polarization ψ. (For the sources targeted here, α and δ are always known to high accuracy, while ψ is usually unknown.) The antenna patterns acquire their time dependence from the sidereal rotation of the Earth; explicit expressions for the F_p's are given in [16–18, 25, 26].

For a continuous wave, the polarizations take the simple form:

$$h_p(t) = a_p \cos(\phi(t) + \phi_p), \tag{2}$$

where a_p is a time-independent strain amplitude, $\phi(t)$ is the intrinsic phase evolution, and ϕ_p a phase offset for each polarization. The nature of these three quantities depends on the specifics of the underlying theory of gravity and the associated emission mechanism (for different emission mechanisms within GR, see e.g. [27–29]). While we treat a_p and ϕ_p as free parameters, we take $\phi(t)$ to be the same as in the traditional GR analysis [21]:

$$\phi(t) = 2\pi \sum_{j=0}^{N} \frac{\partial_t^{(j)} f_0}{(j+1)!} \left[t - T_0 + \delta t(t)\right]^{(j+1)}, \tag{3}$$

TABLE I. Existing orientation information for pulsars in our band, obtained from observations of the pulsar wind nebulae (see Table 3 in [30], and [31, 32] for measurement details).

	ι	ψ
J0534+2200	$62°.2 \pm 1°.9$	$35°.2 \pm 1°.5$
J0537–6910	$92°.8 \pm 0°.9$	$41°.0 \pm 2°.2$
J0835–4510	$63°.6 \pm 0°.6$	$40°.6 \pm 0°.1$
J1833–1034	$85°.4 \pm 0°.3$	$45° \pm 1°$
J1952+3252	N/A	$-11°.5 \pm 8°.6$

where $\partial_t^{(j)} f_0$ is the $j^{\rm th}$ time derivative of the gravitational-wave frequency measured at the fiducial time T_0; $\delta t(t)$ is the time delay from the observatory to the solar system barycenter (including the known Rømer, Shapiro and Einstein delays), and can also include binary system corrections to transform to the time coordinate to a frame approximately inertial with respect to the source; N is the order of the series expansion (1 or 2 for most sources).

The gravitational-wave frequency f is related to the rotational frequency of the source $f_{\rm rot}$, which is in turn known from electromagnetic observations. Although arbitrary theories of gravity and emission mechanisms may predict gravitational emission at any multiple of the rotational frequency, here we assume $f = 2f_{\rm rot}$, in accordance with the most favored emission model in GR [20]. This restriction arises from practical considerations affecting our specific implementation. However, the constraint can be loosely justified by the expectation that, in most viable theories, conservation laws will still preclude emission at the first harmonic ($f = f_{\rm rot}$), while higher frequencies will be suppressed, as in most multiple expansions. Nevertheless, this assumption will be relaxed in a future study.

For convenience, we define *effective strain amplitudes* for tensor, vector and scalar modes respectively by

$$h_{\rm t} \equiv \sqrt{a_+^2 + a_\times^2}, \tag{4}$$

$$h_{\rm v} \equiv \sqrt{a_{\rm x}^2 + a_{\rm y}^2}, \tag{5}$$

$$h_{\rm s} \equiv a_{\rm s}, \tag{6}$$

in terms of the intrinsic a_p amplitudes of Eq. (2). These quantities may serve as proxy for the total power in each polarization group.

One may recover the GR hypothesis considered in previous analysis by setting:

$$a_+ = h_0(1+\cos^2\iota)/2 \ , \ \phi_+ = \phi_0, \tag{7}$$

$$a_\times = h_0 \cos\iota \ , \ \phi_\times = \phi_0 - \pi/2, \tag{8}$$

$$a_{\rm x} = a_{\rm y} = a_{\rm s} = 0, \tag{9}$$

where ι is the inclination (angle between the line of sight and the spin axis of the source), and h_0, ϕ_0 are free parameters. (As with ψ, ι is unknown for most pulsars.) This corresponds to the standard triaxial-star emission mechanism (see e.g. [33]). We use this parameterization only when we wish to incorporate known orientation information as explained below; otherwise, we parametrize the tensor polarizations directly in terms of a_+, $a_\times$, ϕ_+ and $\phi_\times$.

Templates of the form of Eq. (1), together with appropriate priors, allow us to compute Bayes factors (marginalized likelihood ratios) for the presence of signals in the data vs Gaussian noise. We do this using an extension of the nested sampling implementation presented in [34] (see [17] for details specific to the non-GR polarizations). The Bayes factors corresponding to each signal model may be combined into the odds $\mathcal{O}^{\rm S}_{\rm N}$ that the data contain a continuous signal of any polarization vs Gaussian noise:

$$\mathcal{O}^{\rm S}_{\rm N} = P(\mathcal{H}_{\rm S} \mid \mathbf{B})/P(\mathcal{H}_{\rm N} \mid \mathbf{B}) \ , \tag{10}$$

i.e. the ratio of the posteriors probabilities that the data $\mathbf{B}$ contain a signal of any polarizations ($\mathcal{H}_{\rm S}$) vs just Gaussian noise ($\mathcal{H}_{\rm N}$). We compute these odds by setting model priors such that $P(\mathcal{H}_{\rm S}) = P(\mathcal{H}_{\rm N})$; then, by Bayes' theorem, $\mathcal{O}^{\rm S}_{\rm N} = \mathcal{B}^{\rm S}_{\rm N}$, with the Bayes factor

$$\mathcal{B}^{\rm S}_{\rm N} \equiv P(\mathbf{B} \mid \mathcal{H}_{\rm S})/P(\mathbf{B} \mid \mathcal{H}_{\rm N}). \tag{11}$$

Built into the astrophysical signal hypothesis, $\mathcal{H}_{\rm S}$, is the requirement of coherence across detectors, which must be satisfied by a real GW signal. In order to make the analysis more robust against non-Gaussian instrumental features in the data, we also define an *instrumental feature* hypothesis, $\mathcal{H}_{\rm I}$, that identifies non-Gaussian noise artifacts by their lack of coherence across detectors [21, 35]. In particular, we define $\mathcal{H}_{\rm I}$ to capture Gaussian noise *or* a detector-incoherent signal (i.e. a feature that mimics an astrophysical signal in a single instrument, but is not recovered consistently across the network) in each detector [17]. We may then compare this to $\mathcal{H}_{\rm S}$ by means of the odds $\mathcal{O}^{\rm S}_{\rm I}$. For D detectors, this is given by:

$$\log \mathcal{O}^{\rm S}_{\rm I} = \log \mathcal{B}^{\rm S}_{\rm N} - \sum_{d=1}^{D} \log\left(\mathcal{B}^{{\rm S}_d}_{{\rm N}_d} + 1\right), \tag{12}$$

where $\mathcal{B}^{{\rm S}_d}_{{\rm N}_d}$ is the signal vs noise Bayes factor computed only from data from the $d^{\rm th}$ detector. This choice implicitly assigns prior weight to the models such that $P(\mathcal{H}_{\rm S}) = P(\mathcal{H}_{\rm I}) \times 0.5^D$ [17]. For an in depth analysis of the behavior of the different Bayesian hypotheses considered here, in the presence absence of simulated signals of all polarizations, we again refer the reader to the paper methods [17].

We compute likelihoods by taking source location, frequency and frequency derivatives as known quantities. In computing Bayes factors, we employ priors uniform in the logarithm of amplitude parameters (h_0 or h_p's), since these are the least informative priors for scaling coefficients [36]; we bound these amplitudes to the 10^{-28}–10^{-24} range [37]. On the other hand, flat amplitude priors are used to compute upper limits, to facilitate comparison with published GR results in [21]. In all cases, flat priors are placed over all phase offsets (ϕ_0 and all the ϕ_p's).

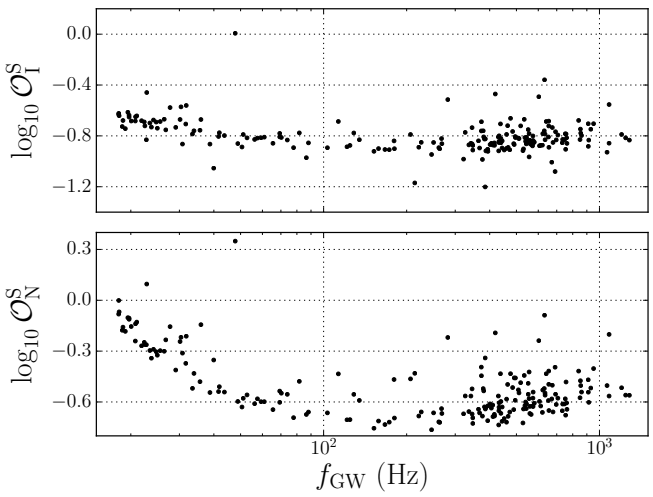

FIG. 1. *Log-odds vs GW frequency.* Log-odds comparing the any-signal hypothesis to the instrumental (top) and Gaussian noise (bottom) hypotheses, as a function of assumed GW frequency, $f = 2f_{\rm rot}$, for each pulsar. Looking at the top plot for $\log \mathcal{O}^{\rm S}_{\rm I}$, notice that the instrumental noise hypothesis is clearly favored for all pulsars except one, for which the analysis is inconclusive. (This is J1932+17, the same non-significant outlier identified in [21].) These results were obtained without incorporating any information on the source orientation, and are tabulated in Table III in the supplementary material. Expressions for both odds are given in Eq. (10) and Eq. (12).

For those few cases in which some orientation information exists (see Table I in supplementary material), we analyze the data a second time using the triaxial parametrization of tensor modes, Eqs. (7) and (8), taking that information into account by marginalizing over ranges of $\cos\iota$ and ψ in agreement with measurement uncertainties.

Results. We find no evidence of continuous-wave signals of any polarization, tensorial or otherwise, from any of the 200 pulsars analyzed. Odds and 95%-credible upper limits are summarized in the supplementary material: Table II, for pulsars with measured orientations (using the triaxial parameterization of tensor modes), and in Table III, for all pulsars without incorporating any orientation information (using the unconstrained parameterization of tensor modes). Odds values are reported with an error of 5% at 90% confidence; errors on the upper limits due to the use of finite samples in estimating posterior probability distributions are at most 10% at 90% confidence,

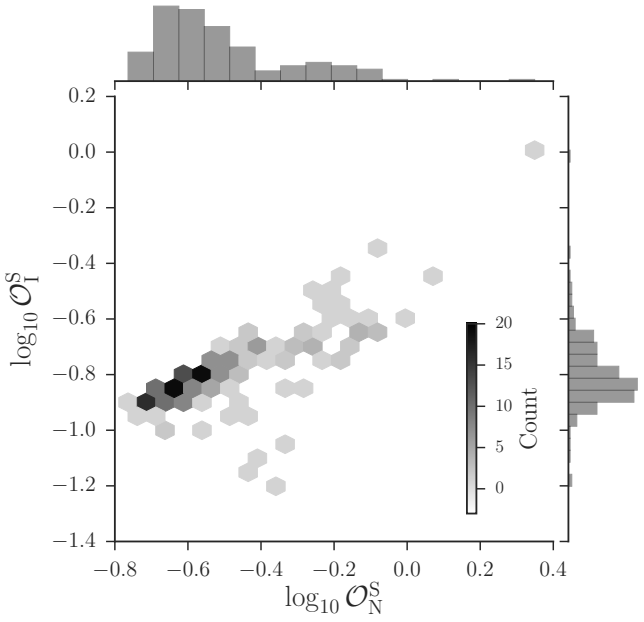

FIG. 2. *Log-odds distributions.* Distributions of log-odds comparing the any-signal hypothesis to the instrumental (ordinate axis, right) and Gaussian noise (abscissa axis, top) hypotheses for all pulsars. This plot contains the same information as Fig. 1 and displays the same non-significant outlier. These results were obtained without incorporating any information on the source orientation, and are tabulated in Table III in the supplementary material. Expressions for both odds in this plot are given in Eq. (10) and Eq. (12). We underscore that, although this plot looks similar to Fig. 2 in [21], the signal hypothesis here incorporates scalar, vector and tensor modes, in all their combinations.

which is slightly less than the 15% error expected from calibration uncertainties.

The main quantity of interest is $\log\mathcal{O}^{\rm S}_{\rm I}$, defined in Eq. (12), since it encodes the probability that the data contain a signal vs just instrumental noise (Gaussian or otherwise). This quantity, together with the log-odds for signal vs Gaussian noise, is presented as a function of assumed GW frequency for each pulsar in Fig. 1, and histogrammed in Fig. 2. Importantly, the outliers in Fig. 1 lose significance once $\log\mathcal{O}^{\rm S}_{\rm I}$ is taken into account; indeed, Figs. 1 and 2 reveal the usefulness of $\log\mathcal{O}^{\rm S}_{\rm I}$ in increasing the robustness of the search against non-Gaussian instrumental artifacts.

Based on the intrinsic probabilistic meaning of $\log\mathcal{O}^{\rm S}_{\rm I}$ in terms of betting odds, it is standard to demand at least $\log\mathcal{O}^{\rm S}_{\rm I} > 1$ to conclude that the signal model is favored (see e.g. the table in Sec. 3.2 of [38], or Jeffrey's original criteria in [39] or [40]). Since none of the odds obtained meet this criterion, we conclude that there is no evidence for signals from any of the pulsars targeted. In most cases, $\log\mathcal{O}^{\rm S}_{\rm I} < 0$ and the noise model is clearly favored; the single exception is J1932+17, for which $\log\mathcal{O}^{\rm S}_{\rm I} \sim 0$, so that we can make no conclusive statement about which hypothesis is preferred. (The presence of this non-significant outlier is to be expected, as it was already identified in [21].)

The distribution of the odds corresponding to the sub-hypotheses making up $\mathcal{H}_{\rm S}$ are summarized in the box plots of Fig. 3. These correspond to tensor-only (t), scalar-only (s), vector-only (v), scalar-vector (sv), scalar-tensor (st), vector-tensor (vt), and scalar-vector-tensor (stv) models. The mean of these distributions decreases with the number of degrees of freedom in the model, which is to be expected from the associated Occam penalties [17]. The right-most panel in Fig. 3 shows the distribution of $\log\mathcal{O}^{\rm S}_{\rm N}$, which results from the combination of all the other odds; this is the same quantity histogrammed on the abscissa of Fig. 2.

In the absence of any discernible signals, we produce upper limits for the magnitude of scalar, vector and tensor polarizations, with a 95% credibility. As usual in Bayesian analyses, upper limits are obtained by integrating posterior probability distributions for the relevant parameters up to the desired credibility (see e.g. [17]). Using the effective amplitude definitions of Eqs. (4)–(6), these quantities are presented in Fig. 4 as a function of assumed GW frequency, and the supplementary material. The plotted upper limits are computed under the assumption of a signal model that includes all five independent polarizations ($\mathcal{H}_{\rm svt}$); limits obtained assuming other signal models may be found online in [41]. Previous work has demonstrated that the presence or absence of a GR component does not affect the non-GR upper limits (Fig. 13 in [17]).

As expected, the upper limits presented here are comparable in magnitude to the upper limits on the GR strain obtained by the traditional searches [21]. However, constraints on the scalar amplitude are, on average, around 20% less stringent than those on the vector or tensor amplitudes. This is a consequence of the fact that, for most source locations in the sky, the LIGO detectors are intrinsically less sensitive to continuous waves of scalar polarization [17].

Technically, traditional all-sky searches for continuous gravitational waves are also sensitive to nontensorial modes, because they are generally designed to look for any signal of sidereal and half-sidereal periodicities in the data [42–44]. However, as can be seen by comparing the magnitude of all-sky upper limits (e.g. Fig. 9 in [42]) to those in shown here in Fig. 4, the sensitivity of these searches would be substantially poorer than that of a targeted search like this one. This is especially true if the search is optimized for a given signal polarization (e.g. circular combination of plus and cross).

Conclusion. We have presented the results of the first direct search for nontensorial gravitational waves. This is also the first search for gravitational waves targeted at known pulsars that is sensitive to any of the six polarizations of the gravitational perturbation allowed by a generic metric theory of gravity. From the analysis of O1 data from both aLIGO observatories, we have found no

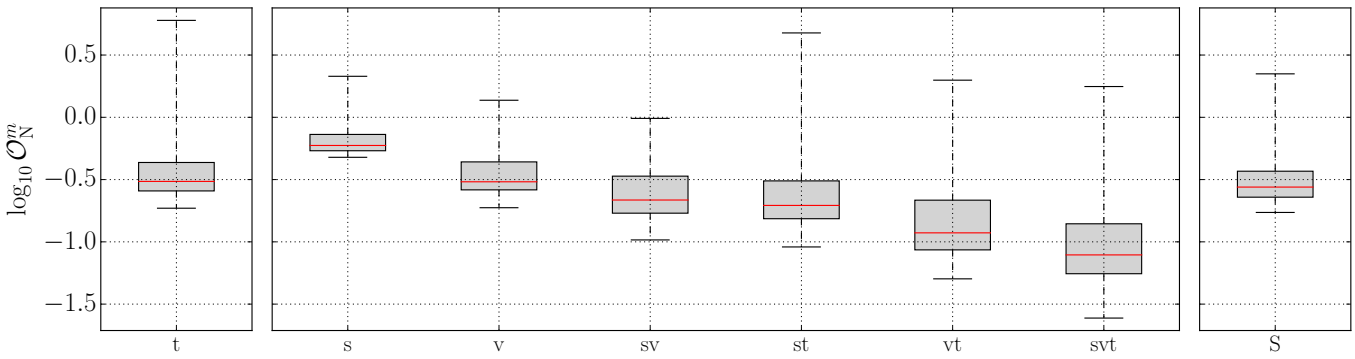

FIG. 3. *Sub-hypothesis odds.* Box plots for the distribution of the signal vs noise log-odds for each of the sub-hypotheses considered, for all of the pulsars analyzed. The sub-hypotheses are: (st), vector-tensor (tv), scalar-vector-tensor tensor-only (t), scalar-only (s), vector-only (v), scalar-vector (sv), scalar-tensor (st), vector-tensor (vt), and scalar-vector-tensor (stv); these are all combined into the signal hypothesis (S). The quantity represented is $\log \mathcal{B}^m_{\rm N}$, which is the same as $\log \mathcal{O}^m_{\rm N}$ if neither $\mathcal{H}_m$ nor $\mathcal{H}_{\rm N}$ are favored *a priori* (hence the label on the ordinate axis). The horizontal red line marks the median of the distribution, while each gray box extends from the lower to upper quartile, and the whiskers mark the full range of the distribution of $\log \mathcal{O}^m_{\rm N}$ for the 200 pulsars analyzed. These results were produced without incorporating any information on the source orientation, and are tabulated in Table III in the supplementary material.

evidence of signals from any of the 200 pulsars targeted.

In the absence of a clear signal, we have produced the first direct upper limits for scalar and vector strains (Fig. 4, and tables in the supplementary material). The values of the 95%-credible upper limits are comparable in magnitude to previously-published GR constraints, reaching $h \sim 1.5 \times 10^{-26}$ for pulsars whose frequency is in the most sensitive band of our instruments.

Our results have been obtained in a model-independent fashion. However, our upper limits on nontensorial strain can be translated into model-dependent constraints by picking a specific alternative theory and emission mechanism. To do so, one should use the upper limits produced under the assumption of a signal model that incorporates the polarizations matching those allowed by the theory one wishes to constrain; these may not necessarily be those in Fig. 4 (e.g. for limits on a scalar-tensor theory, one needs upper limits from $\mathcal{H}_{\rm st}$). However, this also requires non-trivial knowledge of the dynamics of spinning neutron stars under the theory of interest.

While it is conventional to compare the sensitivity of continuous wave searches to the canonical spin-down limit for each pulsar, it is not possible to do so here without committing to a specific theory of gravity. This is because doing so would require specific knowledge of how each polarization contributes to the effective GW stress-energy, how matter couples to the gravitational field, how the waves propagate (dispersion and dissipation), and what the angular dependence of the emission pattern is. However, analogues of the canonical spin-down limit for specific theories may be obtained from the results presented here by using the strain upper limits obtained assuming the sub-hypotheses with polarizations corresponding to that theory, as mentioned above.

We have demonstrated the robustness of searches for generalized polarization states (tensor, vector, or scalar) in gravitational waves from spinning neutron stars. Furthermore, even in the absence of a gravitational-wave detection, we were able to obtain novel constraints on the strain amplitude of nontensorial polarizations. In the future, once a signal is detected, similar methods will allow us to characterize the gravitational polarization content and, in so doing, perform novel tests of general relativity. Although this search assumed a gravitational-wave frequency of twice the rotational frequency of the source, this restriction will be relaxed in future analyses.

Acknowledgments. The authors gratefully acknowledge the support of the United States National Science Foundation (NSF) for the construction and operation of the LIGO Laboratory and Advanced LIGO as well as the Science and Technology Facilities Council (STFC) of the United Kingdom, the Max-Planck-Society (MPS), and the State of Niedersachsen/Germany for support of the construction of Advanced LIGO and construction and operation of the GEO600 detector. Additional support for Advanced LIGO was provided by the Australian Research Council. The authors gratefully acknowledge the Italian Istituto Nazionale di Fisica Nucleare (INFN), the French Centre National de la Recherche Scientifique (CNRS) and the Foundation for Fundamental Research on Matter supported by the Netherlands Organisation for Scientific Research, for the construction and operation of the Virgo detector and the creation and support of the EGO consortium. The authors also gratefully acknowledge research support from these agencies as well as by the Council of Scientific and Industrial Research of India, Department of Science and Technology, India, Science & Engineering Research Board (SERB), India, Ministry of

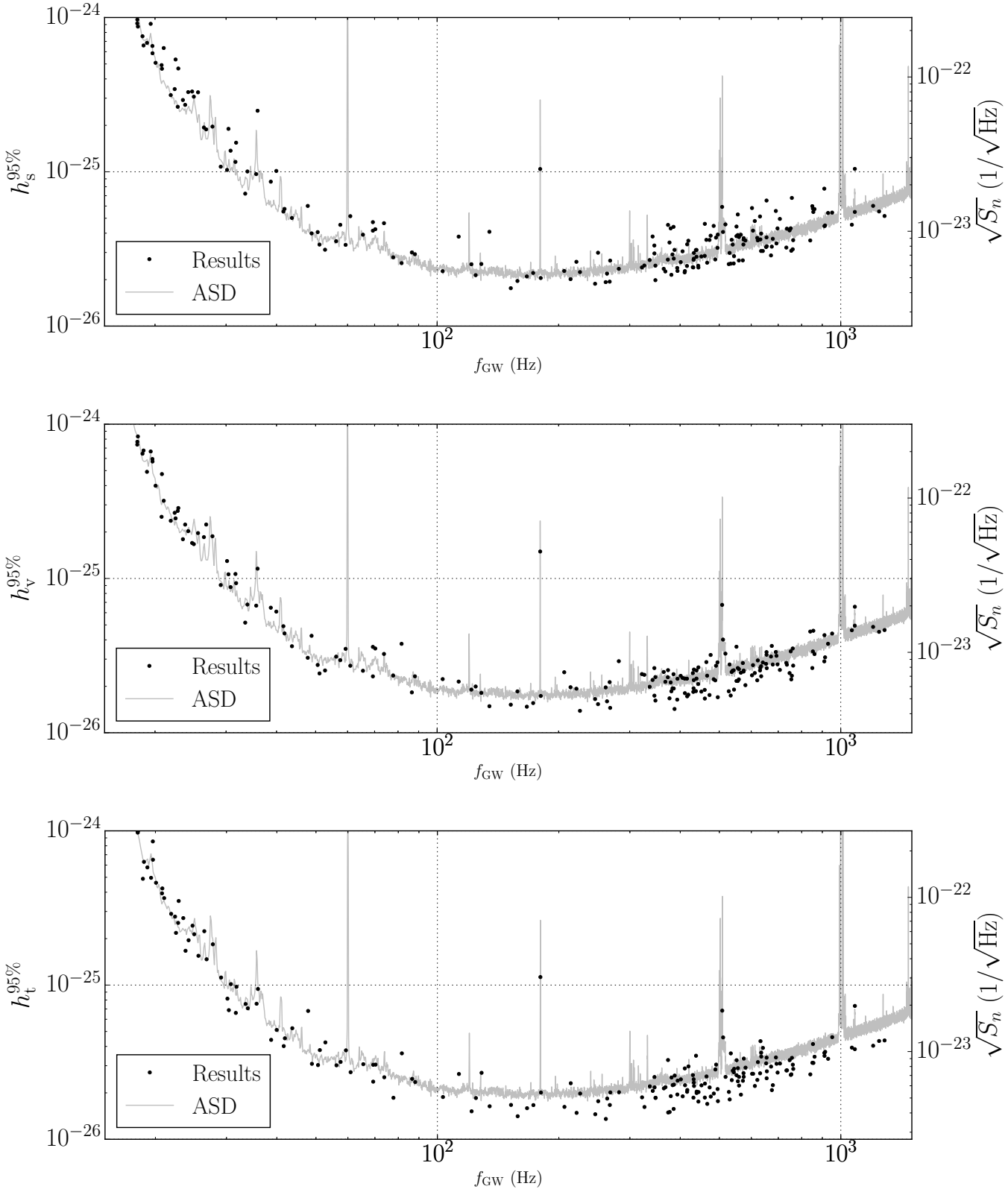

FIG. 4. *Non-GR upper limits vs GW frequency.* Circles mark the 95%-credible upper limit on the scalar, $h_{\rm s}^{95\%}$ (top), and the effective vector, $h_{\rm v}^{95\%}$ (middle), and tensor $h_{\rm t}^{95\%}$ (bottom) strain amplitudes as a function of assumed GW frequency for each of the 200 pulsars in our set. The upper limits are obtained assuming a signal model including all five independent polarizations ($\mathcal{H}_{\rm stv}$), and incorporating no information on the orientation of the source (Table III in supplementary material). The effective amplitude spectral density (ASD) of the detector noise is also displayed for reference; this is the harmonic mean of the H1 and L1 spectra; the scaling is obtained from linear regression to the upper limits.

Human Resource Development, India, the Spanish Ministerio de Economía y Competitividad, the Conselleria d'Economia i Competitivitat and Conselleria d'Educació, Cultura i Universitats of the Govern de les Illes Balears, the National Science Centre of Poland, the European Commission, the Royal Society, the Scottish Funding Council, the Scottish Universities Physics Alliance, the Hungarian Scientific Research Fund (OTKA), the Lyon Institute of Origins (LIO), the National Research Foundation of Korea, Industry Canada and the Province of Ontario through the Ministry of Economic Development and Innovation, the Natural Science and Engineering Research Council Canada, Canadian Institute for Advanced Research, the Brazilian Ministry of Science, Technology, and Innovation, Fundaçao de Amparo à Pesquisa do Estado de São Paulo (FAPESP), Russian Foundation for Basic Research, the Leverhulme Trust, the Research Corporation, Ministry of Science and Technology (MOST), Taiwan and the Kavli Foundation. The authors gratefully acknowledge the support of the NSF, STFC, MPS, INFN, CNRS and the State of Niedersachsen/Germany for provision of computational resources. This paper carries LIGO Document Number LIGO-P1700009.

TABLE II: Results obtained using orientation information (see text for details).

	$f_{\rm GW}$ (Hz)	$\log \mathcal{B}^{\rm GR}_{\rm N}$	$\log \mathcal{B}^{\rm GR+s}_{\rm N}$	$\log \mathcal{B}^{\rm GR+v}_{\rm N}$	$\log \mathcal{B}^{\rm GR+sv}_{\rm N}$	$\log \mathcal{B}^{\rm s}_{\rm N}$	$\log \mathcal{B}^{\rm v}_{\rm N}$	$\log \mathcal{B}^{\rm sv}_{\rm N}$	$\log \mathcal{O}^{\rm S}_{\rm N}$	$\log \mathcal{O}^{\rm S}_{\rm I}$	$h_{\rm s}^{95\%}$	$h_{\rm v}^{95\%}$ $(\times 10^{-26})$	$h_{\rm t}^{95\%}$
J0205+6449	30.41	-0.19	-0.07	-0.32	-0.26	0.06	-0.09	-0.10	-0.12	-0.53	14.79	7.99	3.70
J0534+2200	59.33	-0.19	-0.40	-0.76	-0.88	-0.25	-0.55	-0.74	-0.47	-0.74	1.74	1.69	2.99
J0835-4510	22.37	-0.06	-0.15	-0.29	-0.37	-0.07	-0.21	-0.26	-0.19	-0.67	16.66	13.78	15.27
J1709-4429	19.51	-0.07	-0.02	-0.10	-0.07	0.01	-0.05	-0.04	-0.05	-0.60	61.33	36.31	34.34
J1952+3252	50.59	-0.24	-0.43	-0.81	-0.98	-0.23	-0.58	-0.77	-0.50	-0.80	2.00	1.53	1.49
J2229+6114	38.72	-0.24	-0.40	-0.62	-0.77	-0.19	-0.45	-0.61	-0.43	-0.81	3.36	2.70	2.92

TABLE III: Results obtained without using orientation information (see text for details).

	$f_{\rm GW}$ (Hz)	$\log \mathcal{B}^{\rm s}_{\rm N}$	$\log \mathcal{B}^{\rm v}_{\rm N}$	$\log \mathcal{B}^{\rm t}_{\rm N}$	$\log \mathcal{B}^{\rm sv}_{\rm N}$	$\log \mathcal{B}^{\rm st}_{\rm N}$	$\log \mathcal{B}^{\rm vt}_{\rm N}$	$\log \mathcal{B}^{\rm svt}_{\rm N}$	$\log \mathcal{O}^{\rm S}_{\rm N}$	$\log \mathcal{O}^{\rm S}_{\rm I}$	$h_{\rm s}^{95\%}$	$h_{\rm v}^{95\%}$ $(\times 10^{-26})$	$h_{\rm t}^{95\%}$
J0023+0923	655.69	-0.27	-0.57	-0.56	-0.76	-0.79	-1.05	-1.24	-0.65	-0.89	3.30	2.62	2.76
J0024-7204AA	1083.79	0.07	-0.27	-0.17	-0.21	-0.14	-0.47	-0.46	-0.20	-0.55	10.44	6.56	7.33
J0024-7204AB	539.86	-0.25	-0.55	-0.49	-0.72	-0.70	-0.93	-1.08	-0.60	-0.84	3.38	2.53	2.78
J0024-7204C	347.42	-0.29	-0.68	-0.62	-0.86	-0.92	-1.24	-1.49	-0.73	-0.91	2.46	1.62	1.86
J0024-7204D	373.30	-0.05	-0.32	-0.69	-0.28	-0.76	-0.89	-0.92	-0.45	-0.69	4.53	2.55	1.49
J0024-7204E	565.56	-0.24	-0.57	-0.64	-0.74	-0.92	-1.12	-1.38	-0.67	-0.87	3.91	2.45	1.95
J0024-7204F	762.32	-0.25	-0.58	-0.53	-0.78	-0.78	-1.07	-1.23	-0.64	-0.86	3.60	2.72	2.86
J0024-7204G	495.00	-0.28	-0.38	-0.61	-0.57	-0.88	-0.84	-1.16	-0.59	-0.81	3.21	2.86	2.12
J0024-7204H	622.99	-0.24	-0.47	-0.37	-0.66	-0.60	-0.79	-1.01	-0.53	-0.78	3.59	2.94	3.16
J0024-7204I	573.89	-0.26	-0.51	-0.42	-0.73	-0.65	-0.89	-1.11	-0.58	-0.80	3.38	2.50	2.68
J0024-7204J	952.09	-0.22	-0.36	-0.22	-0.51	-0.49	-0.54	-0.69	-0.40	-0.70	5.44	4.40	4.60
J0024-7204L	460.18	-0.27	-0.64	-0.65	-0.85	-0.93	-1.22	-1.45	-0.72	-0.90	2.85	1.90	1.86
J0024-7204M	543.97	-0.28	-0.66	-0.39	-0.84	-0.63	-0.93	-1.19	-0.61	-0.81	2.84	1.90	2.86
J0024-7204N	654.89	0.02	-0.43	-0.56	-0.35	-0.53	-0.93	-0.92	-0.42	-0.68	6.51	3.20	2.49
J0024-7204O	756.62	-0.06	-0.63	-0.41	-0.58	-0.49	-0.95	-0.98	-0.48	-0.79	6.77	2.34	3.37
J0024-7204Q	495.89	0.02	-0.56	-0.56	-0.45	-0.56	-1.05	-0.97	-0.46	-0.81	3.92	1.70	1.77
J0024-7204R	574.64	-0.24	-0.56	-0.54	-0.72	-0.78	-0.99	-1.26	-0.63	-0.84	3.64	2.50	2.54
J0024-7204S	706.61	-0.19	-0.59	-0.46	-0.71	-0.64	-0.97	-1.13	-0.58	-0.79	4.95	2.55	3.10
J0024-7204T	263.56	-0.29	-0.71	-0.60	-0.90	-0.87	-1.17	-1.44	-0.72	-0.90	2.19	1.60	1.84
J0024-7204U	460.53	-0.11	-0.69	-0.53	-0.72	-0.65	-1.11	-1.17	-0.58	-0.79	4.60	1.67	2.30
J0024-7204W	850.22	-0.14	-0.59	-0.52	-0.65	-0.69	-1.04	-1.18	-0.58	-0.83	5.99	2.63	3.13
J0024-7204X	419.15	-0.20	-0.64	0.24	-0.79	-0.00	-0.35	-0.56	-0.19	-0.47	3.57	1.76	2.97
J0024-7204Y	910.47	-0.03	-0.56	-0.44	-0.56	-0.51	-0.96	-0.98	-0.47	-0.70	7.78	2.90	3.63
J0024-7204Z	439.13	-0.27	-0.53	-0.62	-0.74	-0.89	-1.09	-1.33	-0.67	-0.85	2.81	2.24	2.00
J0030+0451	411.06	-0.29	-0.67	-0.53	-0.84	-0.85	-1.08	-1.34	-0.69	-0.86	2.27	1.81	2.24
J0034-0534	1065.43	-0.23	-0.32	-0.49	-0.48	-0.70	-0.77	-0.96	-0.50	-0.93	4.54	4.62	3.93
J0102+4839	674.74	-0.25	-0.18	-0.63	-0.43	-0.88	-0.82	-0.98	-0.50	-0.73	3.27	3.65	2.08
J0205+6449	30.41	0.06	-0.09	-0.42	-0.10	-0.30	-0.52	-0.53	-0.22	-0.57	18.98	10.65	6.87
J0218+4232	860.92	-0.15	-0.53	-0.48	-0.62	-0.60	-0.94	-1.10	-0.54	-0.80	5.73	3.24	3.43
J0340+4130	606.18	-0.20	-0.57	-0.54	-0.69	-0.72	-0.97	-1.17	-0.60	-0.88	4.16	2.74	2.66
J0348+0432	51.12	-0.26	-0.61	-0.35	-0.79	-0.64	-0.89	-1.09	-0.58	-0.79	3.38	2.42	3.79

Continued on next page

TABLE III: Results obtained without using orientation information (see text for details).

	$f_{\rm GW}$ (Hz)	$\log \mathcal{B}^{\rm s}_{\rm N}$	$\log \mathcal{B}^{\rm v}_{\rm N}$	$\log \mathcal{B}^{\rm t}_{\rm N}$	$\log \mathcal{B}^{\rm sv}_{\rm N}$	$\log \mathcal{B}^{\rm st}_{\rm N}$	$\log \mathcal{B}^{\rm vt}_{\rm N}$	$\log \mathcal{B}^{\rm svt}_{\rm N}$	$\log \mathcal{O}^{\rm S}_{\rm N}$	$\log \mathcal{O}^{\rm S}_{\rm I}$	$h_{\rm s}^{95\%}$	$h_{\rm v}^{95\%}$ $(\times 10^{-26})$	$h_{\rm t}^{95\%}$
J0407+1607	77.82	-0.27	-0.56	-0.68	-0.76	-0.94	-1.15	-1.39	-0.69	-0.89	2.79	2.35	1.86
J0437-4715	347.38	-0.30	-0.53	-0.63	-0.81	-0.93	-1.11	-1.39	-0.69	-0.88	1.98	2.30	1.85
J0453+1559	43.69	-0.23	-0.52	-0.37	-0.70	-0.61	-0.80	-0.99	-0.54	-0.80	5.02	3.64	5.25
J0534+2200	59.33	-0.25	-0.55	-0.48	-0.74	-0.68	-0.91	-1.16	-0.60	-0.82	3.36	3.50	3.77
J0605+37	733.15	-0.26	-0.56	-0.56	-0.79	-0.82	-1.05	-1.25	-0.65	-0.85	3.23	2.84	2.79
J0609+2130	35.91	0.25	-0.32	-0.38	-0.03	-0.10	-0.67	-0.38	-0.14	-0.67	24.86	11.57	9.43
J0610-2100	517.96	-0.08	-0.40	-0.59	-0.44	-0.67	-0.92	-0.99	-0.49	-0.72	4.56	3.26	2.54
J0613-0200	653.20	-0.25	-0.47	-0.52	-0.64	-0.73	-0.97	-1.15	-0.59	-0.81	3.25	2.80	3.11
J0614-3329	635.19	-0.21	-0.58	-0.39	-0.73	-0.62	-0.88	-1.08	-0.56	-0.83	3.98	2.32	3.44
J0621+1002	69.31	-0.22	-0.33	-0.60	-0.48	-0.84	-0.82	-1.02	-0.54	-0.78	4.15	3.60	3.04
J0636+5129	697.12	-0.21	-0.57	-0.54	-0.70	-0.74	-1.04	-1.26	-0.61	-0.83	4.30	2.78	2.71
J0645+5158	225.90	-0.30	-0.71	-0.41	-0.98	-0.72	-1.01	-1.30	-0.66	-0.85	2.24	1.39	1.98
J0711-6830	364.23	-0.28	-0.47	-0.58	-0.70	-0.92	-1.05	-1.24	-0.64	-0.84	2.35	2.48	2.14
J0721-2038	128.68	-0.28	-0.64	-0.27	-0.84	-0.53	-0.85	-1.11	-0.56	-0.78	2.53	1.81	2.70
J0737-3039A	88.11	-0.27	-0.54	-0.58	-0.80	-0.84	-1.08	-1.27	-0.66	-0.85	2.92	2.32	2.35
J0742+66	693.06	-0.26	-0.45	-0.39	-0.68	-0.67	-0.83	-1.11	-0.55	-0.77	3.43	3.15	3.09
J0751+1807	574.92	-0.23	-0.57	-0.35	-0.72	-0.54	-0.83	-1.10	-0.54	-0.86	3.71	2.53	3.34
J0835-4510	22.37	-0.07	-0.21	-0.18	-0.26	-0.28	-0.39	-0.44	-0.25	-0.69	34.36	26.64	27.79
J0900-3144	180.02	-0.17	-0.36	-0.40	-0.51	-0.61	-0.71	-0.88	-0.47	-0.84	10.42	14.95	11.27
J0908-4913	18.73	-0.06	-0.12	-0.11	-0.17	-0.17	-0.23	-0.29	-0.16	-0.68	65.88	67.51	62.92
J0931-1902	431.22	-0.30	-0.64	-0.68	-0.85	-0.91	-1.23	-1.51	-0.74	-0.92	2.40	1.84	1.86
J0940-5428	22.84	0.07	-0.17	0.26	-0.07	0.26	0.04	0.11	0.10	-0.46	46.73	28.61	35.09
J1012+5307	380.54	-0.31	-0.64	-0.22	-0.84	-0.49	-0.78	-1.07	-0.53	-0.81	2.15	1.86	2.52
J1016-5819	22.77	-0.11	-0.21	-0.16	-0.30	-0.28	-0.39	-0.49	-0.26	-0.83	26.39	27.41	25.31
J1016-5857	18.62	-0.05	-0.12	-0.16	-0.16	-0.21	-0.29	-0.32	-0.18	-0.73	75.57	64.39	48.88
J1017-7156	855.24	-0.21	-0.32	-0.53	-0.48	-0.73	-0.76	-0.94	-0.50	-0.78	5.49	4.58	3.13
J1022+1001	121.56	-0.27	-0.61	-0.68	-0.78	-0.95	-1.16	-1.43	-0.71	-0.89	2.52	1.90	1.52
J1024-0719	387.43	-0.23	-0.70	-0.45	-0.87	-0.67	-1.07	-1.29	-0.63	-0.92	3.12	1.43	2.59
J1028-5819	21.88	-0.10	-0.25	-0.15	-0.32	-0.27	-0.42	-0.49	-0.27	-0.68	31.41	23.66	28.95
J1038+0032	69.32	-0.15	-0.59	-0.60	-0.68	-0.73	-1.11	-1.22	-0.60	-0.81	4.72	2.32	2.36
J1045-4509	267.59	-0.30	-0.41	-0.64	-0.66	-0.95	-1.00	-1.25	-0.64	-0.82	1.94	2.13	1.67
J1055-6028	20.07	-0.07	-0.18	-0.03	-0.23	-0.12	-0.24	-0.27	-0.15	-0.68	50.87	39.90	46.08
J1105-6107	31.65	-0.17	-0.15	-0.42	-0.31	-0.61	-0.55	-0.71	-0.37	-0.71	11.59	10.69	6.60
J1112-6103	30.78	-0.14	-0.32	-0.16	-0.43	-0.29	-0.47	-0.53	-0.31	-0.86	13.70	8.79	10.14
J1122+78	476.01	-0.23	-0.12	-0.63	-0.29	-0.86	-0.67	-0.90	-0.43	-0.66	3.85	3.19	1.89
J1125-6014	760.35	-0.26	-0.50	-0.52	-0.67	-0.77	-0.93	-1.15	-0.61	-0.81	3.15	3.52	3.05
J1142+0119	394.07	-0.30	-0.46	-0.54	-0.73	-0.81	-0.93	-1.20	-0.62	-0.92	2.28	2.24	2.40
J1231-1411	542.91	-0.29	-0.52	-0.52	-0.76	-0.82	-0.98	-1.25	-0.64	-0.86	2.55	2.54	2.72
J1300+1240	321.62	-0.27	-0.53	-0.64	-0.73	-0.94	-1.06	-1.29	-0.67	-0.98	2.40	2.40	1.87
J1302-3258	530.38	-0.25	-0.46	-0.68	-0.71	-0.88	-1.00	-1.31	-0.64	-0.90	2.98	2.77	1.81
J1302-6350	41.87	-0.21	-0.45	-0.40	-0.58	-0.59	-0.76	-0.99	-0.51	-0.78	5.75	4.40	4.52
J1312+0051	473.03	-0.21	-0.65	-0.59	-0.82	-0.80	-1.14	-1.31	-0.66	-0.91	3.62	1.76	2.17
J1327-0755	746.85	-0.22	-0.58	-0.50	-0.75	-0.72	-1.01	-1.23	-0.61	-0.83	4.17	2.44	3.26
J1410-6132	39.96	-0.08	-0.34	-0.29	-0.37	-0.38	-0.61	-0.67	-0.35	-1.05	10.13	6.10	5.12
J1418-6058	18.08	0.08	-0.10	0.00	-0.01	0.11	-0.10	-0.04	-0.00	-0.62	96.91	76.92	97.41
J1446-4701	911.29	-0.24	-0.41	-0.46	-0.60	-0.71	-0.82	-1.01	-0.54	-0.88	4.45	4.29	3.47
J1453+1902	345.29	-0.20	-0.45	-0.43	-0.61	-0.66	-0.76	-0.98	-0.52	-0.74	3.33	2.63	2.53
J1455-3330	250.40	-0.17	-0.69	-0.66	-0.82	-0.77	-1.18	-1.46	-0.66	-0.85	2.99	1.53	1.77
J1509-5850	22.49	-0.02	-0.23	-0.26	-0.24	-0.30	-0.48	-0.48	-0.26	-0.72	53.44	24.53	21.80
J1518+4904	48.86	-0.25	-0.46	-0.54	-0.66	-0.81	-0.91	-1.14	-0.60	-0.86	3.99	4.25	3.09
J1524-5625	25.57	-0.06	-0.22	-0.28	-0.27	-0.37	-0.53	-0.55	-0.30	-0.69	32.75	19.68	15.48
J1531-5610	23.75	-0.11	-0.26	-0.30	-0.33	-0.42	-0.54	-0.63	-0.34	-0.73	27.14	22.35	16.68
J1537+1155	52.76	-0.25	-0.55	-0.36	-0.74	-0.60	-0.86	-1.08	-0.56	-0.82	3.13	2.53	4.25
J1545-4550	559.40	-0.21	-0.55	-0.59	-0.72	-0.78	-1.05	-1.21	-0.63	-0.83	3.78	2.59	2.23
J1551-0658	281.94	-0.28	0.14	-0.49	-0.06	-0.80	-0.18	-0.52	-0.22	-0.51	2.35	2.91	2.02
J1600-3053	555.88	0.11	-0.55	-0.61	-0.43	-0.53	-1.11	-1.02	-0.42	-0.97	5.29	2.63	2.38
J1603-7202	134.75	-0.06	-0.73	-0.62	-0.71	-0.68	-1.30	-1.33	-0.59	-0.83	4.09	1.49	1.64
J1614-2230	634.76	-0.27	-0.57	-0.31	-0.78	-0.55	-0.83	-1.01	-0.55	-0.79	3.07	2.70	3.65

Continued on next page

TABLE III: Results obtained without using orientation information (see text for details).

	$f_{\rm GW}$ (Hz)	$\log \mathcal{B}^{\rm s}_{\rm N}$	$\log \mathcal{B}^{\rm v}_{\rm N}$	$\log \mathcal{B}^{\rm t}_{\rm N}$	$\log \mathcal{B}^{\rm sv}_{\rm N}$	$\log \mathcal{B}^{\rm st}_{\rm N}$	$\log \mathcal{B}^{\rm vt}_{\rm N}$	$\log \mathcal{B}^{\rm svt}_{\rm N}$	$\log \mathcal{O}^{\rm S}_{\rm N}$	$\log \mathcal{O}^{\rm S}_{\rm I}$	$h_{\rm s}^{95\%}$	$h_{\rm v}^{95\%}$ $(\times 10^{-26})$	$h_{\rm t}^{95\%}$
J1618-3921	166.84	-0.30	-0.69	-0.61	-0.91	-0.90	-1.23	-1.51	-0.73	-0.91	2.10	1.48	1.59
J1623-2631	180.57	-0.30	-0.68	-0.52	-0.94	-0.81	-1.06	-1.40	-0.69	-0.90	2.05	1.73	2.01
J1630+37	602.75	0.33	-0.61	-0.58	-0.23	-0.26	-1.12	-0.74	-0.24	-0.49	5.82	2.36	2.66
J1640+2224	632.25	-0.23	-0.54	0.37	-0.69	0.13	-0.23	-0.42	-0.09	-0.36	3.64	2.64	4.33
J1643-1224	432.75	-0.25	-0.48	-0.57	-0.63	-0.81	-0.92	-1.18	-0.61	-0.80	2.98	2.57	2.22
J1653-2054	484.36	-0.03	-0.57	-0.60	-0.53	-0.64	-1.14	-1.09	-0.51	-0.77	4.46	2.22	1.98
J1708-3506	443.94	-0.28	-0.48	-0.59	-0.70	-0.83	-0.94	-1.21	-0.63	-0.84	2.40	2.65	2.02
J1709+2313	431.85	-0.26	-0.62	-0.51	-0.80	-0.77	-1.06	-1.29	-0.65	-0.85	2.69	1.94	2.45
J1709-4429	19.51	0.01	-0.05	-0.15	-0.04	-0.12	-0.22	-0.20	-0.10	-0.61	90.99	66.52	49.59
J1710+49	621.07	-0.23	-0.61	-0.58	-0.78	-0.83	-1.15	-1.33	-0.66	-0.87	3.73	2.19	2.43
J1713+0747	437.62	-0.28	-0.64	-0.09	-0.83	-0.31	-0.66	-0.82	-0.43	-0.71	3.11	1.86	3.48
J1718-3825	26.78	-0.12	-0.03	-0.32	-0.15	-0.42	-0.34	-0.44	-0.23	-0.75	18.84	22.36	14.69
J1719-1438	345.41	-0.25	-0.65	-0.57	-0.85	-0.78	-1.11	-1.33	-0.67	-0.86	2.96	1.74	2.17
J1721-2457	571.98	-0.27	-0.49	-0.54	-0.70	-0.81	-0.97	-1.20	-0.62	-0.88	2.67	2.83	2.39
J1727-2946	73.85	-0.14	-0.51	-0.60	-0.56	-0.72	-0.94	-1.11	-0.55	-0.83	4.64	3.24	2.52
J1729-2117	30.17	-0.17	0.03	-0.38	-0.12	-0.54	-0.32	-0.51	-0.24	-0.67	10.28	12.97	8.17
J1730-2304	246.22	-0.31	-0.66	-0.70	-0.88	-1.04	-1.23	-1.61	-0.76	-0.95	1.88	1.65	1.45
J1731-1847	853.04	-0.15	-0.48	-0.33	-0.61	-0.51	-0.81	-0.89	-0.47	-0.75	5.78	3.37	4.14
J1732-5049	376.47	-0.18	-0.66	-0.70	-0.81	-0.86	-1.26	-1.45	-0.68	-0.99	3.48	1.67	1.50
J1738+0333	341.87	-0.12	-0.52	-0.64	-0.60	-0.74	-1.00	-1.13	-0.57	-0.86	3.81	2.20	2.06
J1741+1351	533.74	-0.29	-0.69	-0.05	-0.88	-0.37	-0.63	-0.91	-0.44	-0.67	2.54	1.74	3.61
J1744-1134	490.85	-0.19	-0.36	-0.35	-0.52	-0.57	-0.70	-0.85	-0.46	-0.87	3.75	2.72	3.05
J1745+1017	754.11	-0.27	-0.59	-0.57	-0.84	-0.85	-1.14	-1.34	-0.68	-0.91	3.08	2.22	2.64
J1745-0952	103.22	-0.30	-0.48	-0.65	-0.74	-0.92	-1.01	-1.28	-0.66	-0.89	2.27	2.23	1.88
J1748-2446A	172.96	-0.29	-0.66	-0.63	-0.89	-0.85	-1.18	-1.46	-0.72	-0.91	2.21	1.56	1.67
J1748-3009	206.53	-0.28	-0.09	-0.61	-0.42	-0.90	-0.69	-0.91	-0.46	-0.79	2.28	2.47	1.62
J1750-2536	57.55	-0.21	-0.53	-0.47	-0.69	-0.69	-0.97	-1.16	-0.58	-0.82	4.53	2.95	3.17
J1751-2857	510.87	-0.22	-0.54	-0.37	-0.72	-0.60	-0.84	-1.08	-0.55	-0.82	4.08	4.02	4.58
J1753-1914	31.77	0.14	-0.33	-0.24	-0.22	-0.18	-0.55	-0.48	-0.21	-0.56	15.43	9.33	9.74
J1753-2240	21.02	0.08	-0.20	-0.14	-0.09	-0.07	-0.36	-0.25	-0.13	-0.64	63.40	31.89	36.62
J1756-2251	70.27	-0.19	-0.47	-0.49	-0.57	-0.71	-0.89	-1.09	-0.55	-0.81	4.24	3.52	3.05
J1757-27	113.08	0.02	-0.63	-0.40	-0.55	-0.41	-1.03	-0.92	-0.43	-0.69	3.80	2.15	2.65
J1801-1417	551.71	-0.18	-0.62	-0.41	-0.77	-0.53	-0.99	-1.04	-0.55	-0.84	4.42	2.17	3.26
J1801-3210	268.33	-0.24	-0.72	-0.51	-0.87	-0.73	-1.16	-1.35	-0.67	-0.86	2.66	1.45	2.01
J1802-2124	158.13	-0.31	-0.53	-0.72	-0.77	-0.99	-1.19	-1.39	-0.71	-0.90	1.96	1.85	1.41
J1804-0735	86.58	-0.26	-0.63	-0.56	-0.85	-0.82	-1.10	-1.32	-0.67	-0.97	3.00	1.83	2.46
J1804-2717	214.06	-0.31	-0.44	-0.15	-0.65	-0.42	-0.56	-0.81	-0.43	-1.17	2.02	1.97	2.31
J1809-1917	24.17	-0.07	-0.24	-0.24	-0.29	-0.33	-0.47	-0.56	-0.29	-0.68	32.86	20.26	19.52
J1810+1744	1202.82	-0.20	-0.35	-0.52	-0.51	-0.72	-0.81	-1.02	-0.52	-0.79	6.01	4.86	4.04
J1811-2405	751.71	-0.21	-0.43	-0.55	-0.62	-0.81	-0.98	-1.19	-0.58	-0.78	4.30	3.37	2.61
J1813-1246	41.60	-0.19	-0.42	-0.55	-0.55	-0.71	-0.83	-1.02	-0.54	-0.80	5.52	4.90	4.02
J1813-2621	451.47	-0.25	-0.69	-0.59	-0.85	-0.88	-1.17	-1.42	-0.70	-0.91	2.83	1.85	2.24
J1823-3021A	367.65	-0.28	-0.57	-0.54	-0.81	-0.83	-1.09	-1.29	-0.66	-0.90	2.26	2.14	2.18
J1824-2452A	654.81	-0.25	-0.47	-0.34	-0.62	-0.56	-0.65	-0.87	-0.50	-0.72	3.76	3.33	3.38
J1825-0319	439.22	-0.24	-0.44	-0.58	-0.62	-0.80	-1.01	-1.17	-0.60	-0.82	3.12	2.53	2.04
J1826-1256	18.14	-0.03	-0.10	-0.01	-0.12	-0.02	-0.09	-0.14	-0.07	-0.64	87.34	83.25	100.73
J1826-1334	19.71	-0.06	-0.10	-0.02	-0.16	-0.10	-0.13	-0.19	-0.11	-0.64	65.37	59.45	85.41
J1828-1101	27.76	-0.11	-0.06	-0.12	-0.17	-0.21	-0.19	-0.27	-0.16	-0.58	19.63	18.77	18.38
J1832-0836	735.53	-0.20	-0.55	-0.55	-0.72	-0.78	-1.02	-1.20	-0.61	-0.83	4.28	2.76	2.80
J1833-0827	23.45	-0.08	-0.28	-0.20	-0.36	-0.29	-0.49	-0.54	-0.30	-0.70	29.20	17.97	27.18
J1837-0604	20.77	-0.08	-0.25	-0.14	-0.28	-0.22	-0.38	-0.45	-0.24	-0.68	49.15	25.10	39.34
J1840-0643	56.21	-0.26	-0.45	-0.58	-0.66	-0.82	-0.94	-1.18	-0.61	-0.83	3.55	3.11	3.02
J1843-1113	1083.62	-0.22	-0.44	-0.52	-0.61	-0.71	-0.90	-1.11	-0.57	-0.86	5.49	4.94	3.84
J1845-0743	19.10	-0.06	-0.14	-0.14	-0.19	-0.21	-0.27	-0.33	-0.18	-0.74	68.50	49.13	57.96
J1853+1303	488.78	-0.29	-0.58	-0.49	-0.79	-0.79	-0.99	-1.26	-0.65	-0.86	2.70	2.19	2.84
J1853-0004	19.72	-0.07	0.00	-0.12	-0.08	-0.19	-0.14	-0.21	-0.11	-0.65	58.67	57.30	64.98
J1856+0245	24.72	-0.09	-0.27	-0.23	-0.33	-0.30	-0.51	-0.57	-0.30	-0.69	33.13	16.98	24.27
J1857+0943	372.99	-0.26	-0.47	-0.09	-0.66	-0.38	-0.51	-0.75	-0.39	-0.76	2.70	2.29	3.27

Continued on next page

TABLE III: Results obtained without using orientation information (see text for details).

	$f_{\rm GW}$ (Hz)	$\log \mathcal{B}^{\rm s}_{\rm N}$	$\log \mathcal{B}^{\rm v}_{\rm N}$	$\log \mathcal{B}^{\rm t}_{\rm N}$	$\log \mathcal{B}^{\rm sv}_{\rm N}$	$\log \mathcal{B}^{\rm st}_{\rm N}$	$\log \mathcal{B}^{\rm vt}_{\rm N}$	$\log \mathcal{B}^{\rm svt}_{\rm N}$	$\log \mathcal{O}^{\rm S}_{\rm N}$	$\log \mathcal{O}^{\rm S}_{\rm I}$	$h_{\rm s}^{95\%}$	$h_{\rm v}^{95\%}$ $(\times 10^{-26})$	$h_{\rm t}^{95\%}$
J1903+0327	930.27	-0.17	-0.39	-0.52	-0.51	-0.69	-0.88	-0.97	-0.52	-0.75	5.41	3.77	3.33
J1903-7051	555.88	-0.23	-0.60	-0.38	-0.78	-0.63	-0.94	-1.15	-0.58	-0.78	3.89	2.17	2.89
J1909-3744	678.63	-0.25	-0.56	-0.61	-0.74	-0.83	-1.10	-1.35	-0.66	-0.85	3.68	2.77	2.24
J1910+1256	401.32	-0.28	-0.49	-0.52	-0.67	-0.80	-0.92	-1.16	-0.61	-0.87	2.60	2.34	2.45
J1910-5959A	612.33	-0.17	-0.57	-0.61	-0.73	-0.81	-1.10	-1.25	-0.62	-0.87	4.80	2.44	2.22
J1910-5959C	378.98	-0.04	-0.56	-0.62	-0.54	-0.63	-1.05	-1.15	-0.52	-0.76	4.30	2.12	1.90
J1910-5959D	221.35	-0.26	-0.54	-0.68	-0.76	-0.96	-1.12	-1.38	-0.68	-0.89	2.61	1.93	1.48
J1911+1347	432.34	-0.26	-0.60	-0.49	-0.77	-0.74	-0.99	-1.21	-0.63	-0.84	2.73	2.20	2.33
J1911-1114	551.61	-0.23	-0.25	-0.59	-0.39	-0.78	-0.75	-0.97	-0.49	-0.75	3.83	3.61	2.60
J1915+1606	33.88	-0.17	-0.34	-0.38	-0.46	-0.49	-0.65	-0.82	-0.43	-0.76	10.05	6.78	7.07
J1918-0642	261.58	-0.30	-0.54	-0.73	-0.77	-0.99	-1.21	-1.51	-0.72	-0.89	1.93	1.97	1.35
J1923+2515	527.96	-0.29	-0.66	-0.63	-0.87	-0.92	-1.21	-1.47	-0.72	-0.92	2.52	1.86	2.03
J1925+1721	26.43	-0.13	-0.26	-0.18	-0.36	-0.35	-0.42	-0.54	-0.30	-0.67	19.36	18.54	22.34
J1928+1746	29.10	-0.15	-0.37	-0.30	-0.49	-0.46	-0.61	-0.78	-0.41	-0.73	10.80	9.07	11.19
J1932+17	47.81	-0.20	-0.52	0.78	-0.71	0.68	0.30	0.25	0.35	0.01	6.01	3.06	6.80
J1935+2025	24.96	-0.09	-0.29	-0.27	-0.33	-0.34	-0.54	-0.61	-0.32	-0.74	30.68	16.69	21.37
J1939+2134	1283.86	-0.23	-0.44	-0.49	-0.60	-0.73	-0.89	-1.10	-0.56	-0.83	5.17	4.63	4.37
J1943+2210	393.38	-0.29	-0.66	-0.57	-0.90	-0.87	-1.20	-1.41	-0.71	-0.90	2.38	1.64	1.95
J1944+0907	385.71	-0.25	-0.60	-0.53	-0.80	-0.77	-0.97	-1.28	-0.64	-0.82	2.74	1.94	2.26
J1946+3417	630.89	-0.05	-0.58	-0.55	-0.57	-0.61	-1.04	-1.12	-0.52	-0.76	5.13	2.53	2.68
J1949+3106	152.23	-0.32	-0.68	-0.66	-0.90	-0.97	-1.19	-1.53	-0.75	-0.92	1.76	1.52	1.67
J1950+2414	464.60	-0.21	-0.34	-0.49	-0.48	-0.68	-0.73	-0.97	-0.50	-0.72	3.62	2.87	2.55
J1952+3252	50.59	-0.23	-0.58	-0.52	-0.77	-0.77	-1.07	-1.24	-0.63	-0.89	4.07	2.75	3.03
J1955+2527	410.44	-0.30	-0.62	-0.38	-0.83	-0.69	-0.94	-1.17	-0.62	-0.87	2.23	2.24	2.88
J1955+2908	326.10	-0.28	-0.26	-0.68	-0.51	-0.92	-0.91	-1.16	-0.56	-0.77	2.47	2.37	1.62
J1959+2048	1244.24	-0.22	-0.48	-0.47	-0.63	-0.70	-0.91	-1.03	-0.56	-0.82	5.53	4.51	4.34
J2007+2722	81.64	-0.30	-0.26	-0.46	-0.48	-0.75	-0.55	-0.85	-0.48	-0.78	2.56	3.77	3.61
J2010-1323	382.90	-0.22	-0.58	-0.54	-0.76	-0.76	-1.05	-1.31	-0.63	-0.82	2.91	1.94	2.24
J2017+0603	690.56	-0.03	-0.44	-0.43	-0.39	-0.40	-0.80	-0.76	-0.39	-1.08	5.57	3.34	3.39
J2019+2425	508.32	-0.22	-0.45	-0.42	-0.60	-0.63	-0.82	-1.02	-0.53	-0.82	5.92	6.74	6.83
J2033+1734	336.19	-0.29	-0.57	-0.52	-0.79	-0.81	-1.08	-1.27	-0.66	-0.87	2.68	1.99	2.20
J2043+1711	840.38	-0.26	-0.08	-0.58	-0.32	-0.83	-0.60	-0.86	-0.42	-0.68	3.59	4.53	2.64
J2043+2740	20.81	-0.05	-0.07	-0.13	-0.13	-0.18	-0.19	-0.25	-0.14	-0.65	46.55	47.49	42.33
J2047+1053	466.64	-0.27	-0.54	-0.65	-0.75	-0.97	-1.15	-1.31	-0.68	-0.89	2.57	2.34	1.70
J2051-0827	443.59	-0.29	-0.60	-0.69	-0.79	-0.93	-1.19	-1.42	-0.71	-0.90	2.46	2.07	1.76
J2124-3358	405.59	-0.24	-0.53	-0.60	-0.69	-0.84	-1.04	-1.27	-0.64	-0.86	3.05	2.27	1.90
J2129+1210A	18.07	-0.00	-0.12	-0.03	-0.12	-0.05	-0.13	-0.15	-0.08	-0.63	91.59	73.71	98.25
J2129+1210B	35.63	-0.18	-0.42	-0.37	-0.56	-0.56	-0.74	-0.94	-0.48	-0.76	9.66	6.67	7.57
J2129+1210C	65.51	-0.25	-0.57	-0.58	-0.75	-0.76	-1.08	-1.25	-0.65	-0.86	3.91	2.52	3.07
J2129+1210D	416.42	-0.22	-0.67	-0.64	-0.80	-0.84	-1.21	-1.34	-0.68	-0.87	3.39	1.72	2.09
J2129+1210E	429.97	-0.28	-0.43	-0.49	-0.62	-0.68	-0.83	-1.09	-0.56	-0.81	2.41	2.43	2.61
J2129-5721	536.72	-0.23	-0.53	-0.55	-0.72	-0.81	-1.02	-1.19	-0.62	-0.81	3.62	2.48	2.42
J2145-0750	124.59	-0.30	-0.53	-0.68	-0.76	-0.98	-1.15	-1.42	-0.70	-0.88	2.14	1.99	1.85
J2214+3000	641.18	-0.27	-0.48	-0.14	-0.70	-0.42	-0.64	-0.77	-0.43	-0.69	3.07	2.85	3.91
J2222-0137	60.94	-0.19	-0.51	-0.61	-0.62	-0.77	-1.06	-1.22	-0.60	-0.81	5.16	2.72	2.72
J2229+2643	671.63	-0.27	-0.41	-0.51	-0.66	-0.78	-0.88	-1.10	-0.58	-1.01	2.87	3.12	2.96
J2229+6114	38.72	-0.19	-0.45	-0.48	-0.61	-0.67	-0.90	-1.06	-0.54	-0.86	8.63	6.46	4.41
J2234+06	559.19	-0.28	-0.60	-0.55	-0.81	-0.82	-1.08	-1.24	-0.67	-0.86	2.66	2.22	2.54
J2235+1506	33.46	-0.21	-0.47	-0.41	-0.60	-0.58	-0.84	-0.98	-0.52	-0.79	7.22	5.17	7.54
J2241-5236	914.62	-0.23	-0.54	-0.51	-0.73	-0.71	-0.95	-1.17	-0.60	-0.83	4.49	3.08	3.69
J2302+4442	385.18	0.21	-0.48	-0.72	-0.27	-0.52	-1.03	-0.90	-0.34	-1.20	4.40	2.40	1.57
J2317+1439	580.51	-0.23	-0.63	-0.43	-0.76	-0.71	-0.99	-1.19	-0.61	-0.85	3.59	2.03	2.91
J2322+2057	415.94	-0.28	-0.52	-0.65	-0.78	-0.86	-1.08	-1.36	-0.67	-0.86	2.45	2.24	2.03

[1] B. P. Abbott et al., (The LIGO Scientific Collaboration, and The Virgo Collaboration), Phys. Rev. Lett. **116**, 061102 (2016).

[2] B. P. Abbott et al., (The LIGO Scientific Collaboration, and The Virgo Collaboration), Phys. Rev. Lett. **116**, 241103 (2016).

[3] B. P. Abbott et al., (The LIGO Scientific Collaboration,

and The Virgo Collaboration), Phys. Rev. X **6**, 041015 (2016), arXiv:1606.04856.
[4] B. P. Abbott, (The LIGO Scientific Collaboration, and The Virgo Collaboration), Phys. Rev. Lett. **118**, 221101 (2017), arXiv:1706.01812.
[5] B. P. Abbott et al., (The LIGO Scientific Collaboration, and The Virgo Collaboration), Phys. Rev. Lett. **116**, 221101 (2016).
[6] D. M. Eardley, D. L. Lee, A. P. Lightman, R. V. Wagoner, and C. M. Will, Phys. Rev. Lett. **30**, 884 (1973).
[7] D. Eardley, D. Lee, and A. Lightman, Phys. Rev. D **8**, 3308 (1973).
[8] C. M. Will, *Theory and experiment in gravitational physics*, revised ed ed. (Cambridge University Press, Cambridge, 1993).
[9] C. M. Will, Living Rev. Relativ. **17** (2014), 10.12942/lrr-2014-4.
[10] E. Berti, E. Barausse, V. Cardoso, L. Gualtieri, P. Pani, U. Sperhake, L. C. Stein, N. Wex, K. Yagi, T. Baker, C. P. Burgess, F. S. Coelho, D. Doneva, A. D. Felice, P. G. Ferreira, P. C. C. Freire, J. Healy, C. Herdeiro, M. Horbatsch, B. Kleihaus, A. Klein, K. Kokkotas, J. Kunz, P. Laguna, R. N. Lang, T. G. F. Li, T. Littenberg, A. Matas, S. Mirshekari, H. Okawa, E. Radu, R. O'Shaughnessy, B. S. Sathyaprakash, C. V. D. Broeck, H. A. Winther, H. Witek, M. E. Aghili, J. Alsing, B. Bolen, L. Bombelli, S. Caudill, L. Chen, J. C. Degollado, R. Fujita, C. Gao, D. Gerosa, S. Kamali, H. O. Silva, J. G. Rosa, L. Sadeghian, M. Sampaio, H. Sotani, and M. Zilhao, Class. Quantum Gravity **32**, 243001 (2015), arXiv:1501.07274.
[11] K. Chatziioannou, N. Yunes, and N. Cornish, Phys. Rev. D **86**, 022004 (2012).
[12] J. M. Weisberg, D. J. Nice, and J. H. Taylor, Astrophys. J. **722**, 1030 (2010), arXiv:1011.0718.
[13] P. C. C. Freire, N. Wex, G. Esposito-Farèse, J. P. W. Verbiest, M. Bailes, B. A. Jacoby, M. Kramer, I. H. Stairs, J. Antoniadis, and G. H. Janssen, Mon. Not. R. Astron. Soc. **423**, 3328 (2012).
[14] I. H. Stairs, Living Rev. Relativ. **6**, 5 (2003).
[15] N. Wex, "Testing Relativistic Gravity with Radio Pulsars," (2014), arXiv:1402.5594.
[16] M. Isi, A. J. Weinstein, C. Mead, and M. Pitkin, Phys. Rev. D **91**, 082002 (2015).
[17] M. Isi, M. Pitkin, and A. J. Weinstein, "Probing Dynamical Gravity with the Polarization of Continuous Gravitational Waves," (2017), in press, arXiv:1703.07530.
[18] A. Nishizawa, A. Taruya, K. Hayama, S. Kawamura, and M.-a. Sakagami, Phys. Rev. D **79**, 082002 (2009).
[19] T. Callister, A. S. Biscoveanu, N. Christensen, M. Isi, A. Matas, O. Minazzoli, T. Regimbau, M. Sakellariadou, J. Tasson, and E. Thrane, "Tests of General Relativity with the Stochastic Gravitational-Wave Background," (2017), arXiv:1704.08373.
[20] K. S. Thorne, in *Three hundred years of gravitation*, edited by S. W. Hawking and W. Israel (Cambridge University Press, Cambridge, 1987) Chap. 9, pp. 330 – 458.
[21] B. P. Abbott et al., (The LIGO Scientific Collaboration, and The Virgo Collaboration), Astrophys. J. **839**, 12 (2017), arXiv:1701.07709.
[22] R. Dupuis and G. Woan, Phys. Rev. D **72**, 102002 (2005), arXiv:0508096 [gr-qc].
[23] B. P. Abbott and (The LIGO Scientific Collaboration), Phys. Rev. D **95**, 062003 (2017), arXiv:1602.03845.
[24] W. Anderson, P. Brady, J. Creighton, and É. Flanagan, Phys. Rev. D **63**, 042003 (2001).
[25] A. Błaut, Phys. Rev. D **85**, 043005 (2012).
[26] E. Poisson and C. M. Will, *Gravity: Newtonian, Post-Newtonian, Relativistic* (Cambridge University Press, 2014).
[27] M. Zimmermann and E. Szedenits, Phys. Rev. D **20**, 351 (1979).
[28] B. J. Owen, L. Lindblom, C. Cutler, B. F. Schutz, A. Vecchio, and N. Andersson, Phys. Rev. D **58**, 084020 (1998), arXiv:9804044 [gr-qc].
[29] R. Bondarescu, S. A. Teukolsky, and I. Wasserman, Phys. Rev. D **79**, 104003 (2009), arXiv:0809.3448.
[30] J. Aasi et al., (The LIGO Scientific Collaboration, and The Virgo Collaboration), Astrophys. J. **785**, 119 (2014), arXiv:1309.4027.
[31] C. Ng and R. W. Romani, Astrophys. J. **601**, 479 (2004), arXiv:0310155 [astro-ph].
[32] C. Ng and R. W. Romani, Astrophys. J. **673**, 411 (2008).
[33] D. I. Jones and N. Andersson, Mon. Not. R. Astron. Soc. **331**, 203 (2002).
[34] M. Pitkin, C. Gill, J. Veitch, E. Macdonald, and G. Woan, J. Phys. Conf. Ser. **363**, 012041 (2012), arXiv:1203.2856.
[35] D. Keitel, R. Prix, M. A. Papa, P. Leaci, and M. Siddiqi, Phys. Rev. D **89**, 064023 (2014), arXiv:1311.5738.
[36] E. Jaynes, IEEE Trans. Syst. Sci. Cybern. **4**, 227 (1968).
[37] The specific range chosen for the amplitude priors has little effect on our results, as explained in Appendix B of [17].
[38] R. E. Kass and A. E. Raftery, J. Am. Stat. Assoc. **90**, 773 (1995).
[39] Jeffreys Harold, *Theory of probability*, 3rd ed. (Clarendon Press, Oxford, 1998).
[40] C. P. Robert, N. Chopin, and J. Rousseau, Stat. Sci. **24**, 191 (2009), arXiv:arXiv:0804.3173v7.
[41] `https://dcc.ligo.org/LIGO-P1700009/public`.
[42] B. P. Abbott, (The LIGO Scientific Collaboration, and The Virgo Collaboration), Phys. Rev. D **94**, 102002 (2016), arXiv:1606.09619.
[43] B. P. Abbott, (The LIGO Scientific Collaboration, and The Virgo Collaboration), Phys. Rev. D **94**, 042002 (2016), arXiv:1605.03233.
[44] J. Aasi, (The LIGO Scientific Collaboration, and The Virgo Collaboration), Phys. Rev. D **90**, 062010 (2014), arXiv:1405.7904 [gr-qc].

Authors

B. P. Abbott,[1] R. Abbott,[1] T. D. Abbott,[2] F. Acernese,[3,4] K. Ackley,[5] C. Adams,[6] T. Adams,[7] P. Addesso,[8] R. X. Adhikari,[1] V. B. Adya,[9] C. Affeldt,[9] M. Afrough,[10] B. Agarwal,[11] M. Agathos,[12] K. Agatsuma,[13] N. Aggarwal,[14] O. D. Aguiar,[15] L. Aiello,[16,17] A. Ain,[18] P. Ajith,[19] G. Allen,[11] A. Allocca,[20,21] P. A. Altin,[22] A. Amato,[23] A. Ananyeva,[1] S. B. Anderson,[1] W. G. Anderson,[24] S. Antier,[25] S. Appert,[1] K. Arai,[1] M. C. Araya,[1] J. S. Areeda,[26] N. Arnaud,[25,27] K. G. Arun,[28] S. Ascenzi,[29,17] G. Ashton,[9] M. Ast,[30] S. M. Aston,[6] P. Astone,[31] P. Aufmuth,[32] C. Aulbert,[9] K. AultONeal,[33] A. Avila-Alvarez,[26] S. Babak,[34] P. Bacon,[35] M. K. M. Bader,[13] S. Bae,[36] P. T. Baker,[37,38] F. Baldaccini,[39,40] G. Ballardin,[27] S. W. Ballmer,[41] S. Banagiri,[42] J. C. Barayoga,[1] S. E. Barclay,[43] B. C. Barish,[1] D. Barker,[44] F. Barone,[3,4] B. Barr,[43] L. Barsotti,[14] M. Barsuglia,[35] D. Barta,[45] J. Bartlett,[44] I. Bartos,[46] R. Bassiri,[47] A. Basti,[20,21] J. C. Batch,[44] C. Baune,[9] M. Bawaj,[48,40] M. Bazzan,[49,50] B. Bécsy,[51] C. Beer,[9] M. Bejger,[52] I. Belahcene,[25] A. S. Bell,[43] B. K. Berger,[1] G. Bergmann,[9] C. P. L. Berry,[53] D. Bersanetti,[54,55] A. Bertolini,[13] J. Betzwieser,[6] S. Bhagwat,[41] R. Bhandare,[56] I. A. Bilenko,[57] G. Billingsley,[1] C. R. Billman,[5] J. Birch,[6] R. Birney,[58] O. Birnholtz,[9] S. Biscans,[14] A. Bisht,[32] M. Bitossi,[27,21] C. Biwer,[41] M. A. Bizouard,[25] J. K. Blackburn,[1] J. Blackman,[59] C. D. Blair,[60] D. G. Blair,[60] R. M. Blair,[44] S. Bloemen,[61] O. Bock,[9] N. Bode,[9] M. Boer,[62] G. Bogaert,[62] A. Bohe,[34] F. Bondu,[63] R. Bonnand,[7] B. A. Boom,[13] R. Bork,[1] V. Boschi,[20,21] S. Bose,[64,18] Y. Bouffanais,[35] A. Bozzi,[27] C. Bradaschia,[21] P. R. Brady,[24] V. B. Braginsky*,[57] M. Branchesi,[65,66] J. E. Brau,[67] T. Briant,[68] A. Brillet,[62] M. Brinkmann,[9] V. Brisson,[25] P. Brockill,[24] J. E. Broida,[69] A. F. Brooks,[1] D. A. Brown,[41] D. D. Brown,[53] N. M. Brown,[14] S. Brunett,[1] C. C. Buchanan,[2] A. Buikema,[14] T. Bulik,[70] H. J. Bulten,[71,13] A. Buonanno,[34,72] D. Buskulic,[7] C. Buy,[35] R. L. Byer,[47] M. Cabero,[9] L. Cadonati,[73] G. Cagnoli,[23,74] C. Cahillane,[1] J. Calderón Bustillo,[73] T. A. Callister,[1] E. Calloni,[75,4] J. B. Camp,[76] M. Canepa,[54,55] P. Canizares,[61] K. C. Cannon,[77] H. Cao,[78] J. Cao,[79] C. D. Capano,[9] E. Capocasa,[35] F. Carbognani,[27] S. Caride,[80] M. F. Carney,[81] J. Casanueva Diaz,[25] C. Casentini,[29,17] S. Caudill,[24] M. Cavaglià,[10] F. Cavalier,[25] R. Cavalieri,[27] G. Cella,[21] C. B. Cepeda,[1] L. Cerboni Baiardi,[65,66] G. Cerretani,[20,21] E. Cesarini,[29,17] S. J. Chamberlin,[82] M. Chan,[43] S. Chao,[83] P. Charlton,[84] E. Chassande-Mottin,[35] D. Chatterjee,[24] B. D. Cheeseboro,[37,38] H. Y. Chen,[85] Y. Chen,[59] H.-P. Cheng,[5] A. Chincarini,[55] A. Chiummo,[27] T. Chmiel,[81] H. S. Cho,[86] M. Cho,[72] J. H. Chow,[22] N. Christensen,[69,62] Q. Chu,[60] A. J. K. Chua,[12] S. Chua,[68] A. K. W. Chung,[87] S. Chung,[60] G. Ciani,[5] R. Ciolfi,[88,89] C. E. Cirelli,[47] A. Cirone,[54,55] F. Clara,[44] J. A. Clark,[73] F. Cleva,[62] C. Cocchieri,[10] E. Coccia,[16,17] P.-F. Cohadon,[68] A. Colla,[90,31] C. G. Collette,[91] L. R. Cominsky,[92] M. Constancio Jr.,[15] L. Conti,[50] S. J. Cooper,[53] P. Corban,[6] T. R. Corbitt,[2] K. R. Corley,[46] N. Cornish,[93] A. Corsi,[80] S. Cortese,[27] C. A. Costa,[15] M. W. Coughlin,[69] S. B. Coughlin,[94,95] J.-P. Coulon,[62] S. T. Countryman,[46] P. Couvares,[1] P. B. Covas,[96] E. E. Cowan,[73] D. M. Coward,[60] M. J. Cowart,[6] D. C. Coyne,[1] R. Coyne,[80] J. D. E. Creighton,[24] T. D. Creighton,[97] J. Cripe,[2] S. G. Crowder,[98] T. J. Cullen,[26] A. Cumming,[43] L. Cunningham,[43] E. Cuoco,[27] T. Dal Canton,[76] S. L. Danilishin,[32,9] S. D'Antonio,[17] K. Danzmann,[32,9] A. Dasgupta,[99] C. F. Da Silva Costa,[5] V. Dattilo,[27] I. Dave,[56] M. Davier,[25] D. Davis,[41] E. J. Daw,[100] B. Day,[73] S. De,[41] D. DeBra,[47] J. Degallaix,[23] M. De Laurentis,[75,4] S. Deléglise,[68] W. Del Pozzo,[53,20,21] T. Denker,[9] T. Dent,[9] V. Dergachev,[34] R. De Rosa,[75,4] R. T. DeRosa,[6] R. DeSalvo,[101] J. Devenson,[58] R. C. Devine,[37,38] S. Dhurandhar,[18] M. C. Díaz,[97] L. Di Fiore,[4] M. Di Giovanni,[102,89] T. Di Girolamo,[75,4,46] A. Di Lieto,[20,21] S. Di Pace,[90,31] I. Di Palma,[90,31] F. Di Renzo,[20,21] Z. Doctor,[85] V. Dolique,[23] F. Donovan,[14] K. L. Dooley,[10] S. Doravari,[9] I. Dorrington,[95] R. Douglas,[43] M. Dovale Álvarez,[53] T. P. Downes,[24] M. Drago,[9] R. W. P. Drever‡,[1] J. C. Driggers,[44] Z. Du,[79] M. Ducrot,[7] J. Duncan,[94] S. E. Dwyer,[44] T. B. Edo,[100] M. C. Edwards,[69] A. Effler,[6] H.-B. Eggenstein,[9] P. Ehrens,[1] J. Eichholz,[1] S. S. Eikenberry,[5] R. A. Eisenstein,[14] R. C. Essick,[14] Z. B. Etienne,[37,38] T. Etzel,[1] M. Evans,[14] T. M. Evans,[6] M. Factourovich,[46] V. Fafone,[29,17,16] H. Fair,[41] S. Fairhurst,[95] X. Fan,[79] S. Farinon,[55] B. Farr,[85] W. M. Farr,[53] E. J. Fauchon-Jones,[95] M. Favata,[103] M. Fays,[95] H. Fehrmann,[9] J. Feicht,[1] M. M. Fejer,[47] A. Fernandez-Galiana,[14] I. Ferrante,[20,21] E. C. Ferreira,[15] F. Ferrini,[27] F. Fidecaro,[20,21] I. Fiori,[27] D. Fiorucci,[35] R. P. Fisher,[41] R. Flaminio,[23,104] M. Fletcher,[43] H. Fong,[105] P. W. F. Forsyth,[22] S. S. Forsyth,[73] J.-D. Fournier,[62] S. Frasca,[90,31] F. Frasconi,[21] Z. Frei,[51] A. Freise,[53] R. Frey,[67] V. Frey,[25] E. M. Fries,[1] P. Fritschel,[14] V. V. Frolov,[6] P. Fulda,[5,76] M. Fyffe,[6] H. Gabbard,[9] M. Gabel,[106] B. U. Gadre,[18] S. M. Gaebel,[53] J. R. Gair,[107] L. Gammaitoni,[39] M. R. Ganija,[78] S. G. Gaonkar,[18] F. Garufi,[75,4] S. Gaudio,[33] G. Gaur,[108] V. Gayathri,[109] N. Gehrels†,[76] G. Gemme,[55] E. Genin,[27] A. Gennai,[21] D. George,[11] J. George,[56] L. Gergely,[110] V. Germain,[7] S. Ghonge,[73] Abhirup Ghosh,[19] Archisman Ghosh,[19,13] S. Ghosh,[61,13] J. A. Giaime,[2,6] K. D. Giardina,[6] A. Giazotto,[21] K. Gill,[33] L. Glover,[101] E. Goetz,[9] R. Goetz,[5] S. Gomes,[95] G. González,[2] J. M. Gonzalez Castro,[20,21] A. Gopakumar,[111] M. L. Gorodetsky,[57] S. E. Gossan,[1] M. Gosselin,[27]

R. Gouaty,[7] A. Grado,[112,4] C. Graef,[43] M. Granata,[23] A. Grant,[43] S. Gras,[14] C. Gray,[44] G. Greco,[65,66] A. C. Green,[53] P. Groot,[61] H. Grote,[9] S. Grunewald,[34] P. Gruning,[25] G. M. Guidi,[65,66] X. Guo,[79] A. Gupta,[82] M. K. Gupta,[99] K. E. Gushwa,[1] E. K. Gustafson,[1] R. Gustafson,[113] B. R. Hall,[64] E. D. Hall,[1] G. Hammond,[43] M. Haney,[111] M. M. Hanke,[9] J. Hanks,[44] C. Hanna,[82] O. A. Hannuksela,[87] J. Hanson,[6] T. Hardwick,[2] J. Harms,[65,66] G. M. Harry,[114] I. W. Harry,[34] M. J. Hart,[43] C.-J. Haster,[105] K. Haughian,[43] J. Healy,[115] A. Heidmann,[68] M. C. Heintze,[6] H. Heitmann,[62] P. Hello,[25] G. Hemming,[27] M. Hendry,[43] I. S. Heng,[43] J. Hennig,[43] J. Henry,[115] A. W. Heptonstall,[1] M. Heurs,[9,32] S. Hild,[43] D. Hoak,[27] D. Hofman,[23] K. Holt,[6] D. E. Holz,[85] P. Hopkins,[95] C. Horst,[24] J. Hough,[43] E. A. Houston,[43] E. J. Howell,[60] Y. M. Hu,[9] E. A. Huerta,[11] D. Huet,[25] B. Hughey,[33] S. Husa,[96] S. H. Huttner,[43] T. Huynh-Dinh,[6] N. Indik,[9] D. R. Ingram,[44] R. Inta,[80] G. Intini,[90,31] H. N. Isa,[43] J.-M. Isac,[68] M. Isi,[1] B. R. Iyer,[19] K. Izumi,[44] T. Jacqmin,[68] K. Jani,[73] P. Jaranowski,[116] S. Jawahar,[117] F. Jiménez-Forteza,[96] W. W. Johnson,[2] D. I. Jones,[118] R. Jones,[43] R. J. G. Jonker,[13] L. Ju,[60] J. Junker,[9] C. V. Kalaghatgi,[95] V. Kalogera,[94] S. Kandhasamy,[6] G. Kang,[36] J. B. Kanner,[1] S. Karki,[67] K. S. Karvinen,[9] M. Kasprzack,[2] M. Katolik,[11] E. Katsavounidis,[14] W. Katzman,[6] S. Kaufer,[32] K. Kawabe,[44] F. Kéfélian,[62] D. Keitel,[43] A. J. Kemball,[11] R. Kennedy,[100] C. Kent,[95] J. S. Key,[119] F. Y. Khalili,[57] I. Khan,[16,17] S. Khan,[9] Z. Khan,[99] E. A. Khazanov,[120] N. Kijbunchoo,[44] Chunglee Kim,[121] J. C. Kim,[122] W. Kim,[78] W. S. Kim,[123] Y.-M. Kim,[86,121] S. J. Kimbrell,[73] E. J. King,[78] P. J. King,[44] R. Kirchhoff,[9] J. S. Kissel,[44] L. Kleybolte,[30] S. Klimenko,[5] P. Koch,[9] S. M. Koehlenbeck,[9] S. Koley,[13] V. Kondrashov,[1] A. Kontos,[14] M. Korobko,[30] W. Z. Korth,[1] I. Kowalska,[70] D. B. Kozak,[1] C. Krämer,[9] V. Kringel,[9] B. Krishnan,[9] A. Królak,[124,125] G. Kuehn,[9] P. Kumar,[105] R. Kumar,[99] S. Kumar,[19] L. Kuo,[83] A. Kutynia,[124] S. Kwang,[24] B. D. Lackey,[34] K. H. Lai,[87] M. Landry,[44] R. N. Lang,[24] J. Lange,[115] B. Lantz,[47] R. K. Lanza,[14] A. Lartaux-Vollard,[25] P. D. Lasky,[126] M. Laxen,[6] A. Lazzarini,[1] C. Lazzaro,[50] P. Leaci,[90,31] S. Leavey,[43] C. H. Lee,[86] H. K. Lee,[127] H. M. Lee,[121] H. W. Lee,[122] K. Lee,[43] J. Lehmann,[9] A. Lenon,[37,38] M. Leonardi,[102,89] N. Leroy,[25] N. Letendre,[7] Y. Levin,[126] T. G. F. Li,[87] A. Libson,[14] T. B. Littenberg,[128] J. Liu,[60] R. K. L. Lo,[87] N. A. Lockerbie,[117] L. T. London,[95] J. E. Lord,[41] M. Lorenzini,[16,17] V. Loriette,[129] M. Lormand,[6] G. Losurdo,[21] J. D. Lough,[9,32] C. O. Lousto,[115] G. Lovelace,[26] H. Lück,[32,9] D. Lumaca,[29,17] A. P. Lundgren,[9] R. Lynch,[14] Y. Ma,[59] S. Macfoy,[58] B. Machenschalk,[9] M. MacInnis,[14] D. M. Macleod,[2] I. Magaña Hernandez,[87] F. Magaña-Sandoval,[41] L. Magaña Zertuche,[41] R. M. Magee,[82] E. Majorana,[31] I. Maksimovic,[129] N. Man,[62] V. Mandic,[42] V. Mangano,[43] G. L. Mansell,[22] M. Manske,[24] M. Mantovani,[27] F. Marchesoni,[48,40] F. Marion,[7] S. Márka,[46] Z. Márka,[46] C. Markakis,[11] A. S. Markosyan,[47] E. Maros,[1] F. Martelli,[65,66] L. Martellini,[62] I. W. Martin,[43] D. V. Martynov,[14] K. Mason,[14] A. Masserot,[7] T. J. Massinger,[1] M. Masso-Reid,[43] S. Mastrogiovanni,[90,31] A. Matas,[42] F. Matichard,[14] L. Matone,[46] N. Mavalvala,[14] N. Mazumder,[64] R. McCarthy,[44] D. E. McClelland,[22] S. McCormick,[6] L. McCuller,[14] S. C. McGuire,[130] G. McIntyre,[1] J. McIver,[1] D. J. McManus,[22] T. McRae,[22] S. T. McWilliams,[37,38] D. Meacher,[82] G. D. Meadors,[34,9] J. Meidam,[13] E. Mejuto-Villa,[8] A. Melatos,[131] G. Mendell,[44] R. A. Mercer,[24] E. L. Merilh,[44] M. Merzougui,[62] S. Meshkov,[1] C. Messenger,[43] C. Messick,[82] R. Metzdorff,[68] P. M. Meyers,[42] F. Mezzani,[31,90] H. Miao,[53] C. Michel,[23] H. Middleton,[53] E. E. Mikhailov,[132] L. Milano,[75,4] A. L. Miller,[5] A. Miller,[90,31] B. B. Miller,[94] J. Miller,[14] M. Millhouse,[93] O. Minazzoli,[62] Y. Minenkov,[17] J. Ming,[34] C. Mishra,[133] S. Mitra,[18] V. P. Mitrofanov,[57] G. Mitselmakher,[5] R. Mittleman,[14] A. Moggi,[21] M. Mohan,[27] S. R. P. Mohapatra,[14] M. Montani,[65,66] B. C. Moore,[103] C. J. Moore,[12] D. Moraru,[44] G. Moreno,[44] S. R. Morriss,[97] B. Mours,[7] C. M. Mow-Lowry,[53] G. Mueller,[5] A. W. Muir,[95] Arunava Mukherjee,[9] D. Mukherjee,[24] S. Mukherjee,[97] N. Mukund,[18] A. Mullavey,[6] J. Munch,[78] E. A. M. Muniz,[41] P. G. Murray,[43] K. Napier,[73] I. Nardecchia,[29,17] L. Naticchioni,[90,31] R. K. Nayak,[134] G. Nelemans,[61,13] T. J. N. Nelson,[6] M. Neri,[54,55] M. Nery,[9] A. Neunzert,[113] J. M. Newport,[114] G. Newton‡,[43] K. K. Y. Ng,[87] T. T. Nguyen,[22] D. Nichols,[61] A. B. Nielsen,[9] S. Nissanke,[61,13] A. Nitz,[9] A. Noack,[9] F. Nocera,[27] D. Nolting,[6] M. E. N. Normandin,[97] L. K. Nuttall,[41] J. Oberling,[44] E. Ochsner,[24] E. Oelker,[14] G. H. Ogin,[106] J. J. Oh,[123] S. H. Oh,[123] F. Ohme,[9] M. Oliver,[96] P. Oppermann,[9] Richard J. Oram,[6] B. O'Reilly,[6] R. Ormiston,[42] L. F. Ortega,[5] R. O'Shaughnessy,[115] D. J. Ottaway,[78] H. Overmier,[6] B. J. Owen,[80] A. E. Pace,[82] J. Page,[128] M. A. Page,[60] A. Pai,[109] S. A. Pai,[56] J. R. Palamos,[67] O. Palashov,[120] C. Palomba,[31] A. Pal-Singh,[30] H. Pan,[83] B. Pang,[59] P. T. H. Pang,[87] C. Pankow,[94] F. Pannarale,[95] B. C. Pant,[56] F. Paoletti,[21] A. Paoli,[27] M. A. Papa,[34,24,9] H. R. Paris,[47] W. Parker,[6] D. Pascucci,[43] A. Pasqualetti,[27] R. Passaquieti,[20,21] D. Passuello,[21] B. Patricelli,[135,21] B. L. Pearlstone,[43] M. Pedraza,[1] R. Pedurand,[23,136] L. Pekowsky,[41] A. Pele,[6] S. Penn,[137] C. J. Perez,[44] A. Perreca,[1,102,89] L. M. Perri,[94] H. P. Pfeiffer,[105] M. Phelps,[43] O. J. Piccinni,[90,31] M. Pichot,[62] F. Piergiovanni,[65,66] V. Pierro,[8] G. Pillant,[27] L. Pinard,[23] I. M. Pinto,[8] M. Pitkin,[43] R. Poggiani,[20,21] P. Popolizio,[27] E. K. Porter,[35] A. Post,[9] J. Powell,[43] J. Prasad,[18] J. W. W. Pratt,[33] V. Predoi,[95] T. Prestegard,[24]

M. Prijatelj,[9] M. Principe,[8] S. Privitera,[34] R. Prix,[9] G. A. Prodi,[102,89] L. G. Prokhorov,[57] O. Puncken,[9] M. Punturo,[40] P. Puppo,[31] M. Pürrer,[34] H. Qi,[24] J. Qin,[60] S. Qiu,[126] V. Quetschke,[97] E. A. Quintero,[1] R. Quitzow-James,[67] F. J. Raab,[44] D. S. Rabeling,[22] H. Radkins,[44] P. Raffai,[51] S. Raja,[56] C. Rajan,[56] M. Rakhmanov,[97] K. E. Ramirez,[97] P. Rapagnani,[90,31] V. Raymond,[34] M. Razzano,[20,21] J. Read,[26] T. Regimbau,[62] L. Rei,[55] S. Reid,[58] D. H. Reitze,[1,5] H. Rew,[132] S. D. Reyes,[41] F. Ricci,[90,31] P. M. Ricker,[11] S. Rieger,[9] K. Riles,[113] M. Rizzo,[115] N. A. Robertson,[1,43] R. Robie,[43] F. Robinet,[25] A. Rocchi,[17] L. Rolland,[7] J. G. Rollins,[1] V. J. Roma,[67] R. Romano,[3,4] C. L. Romel,[44] J. H. Romie,[6] D. Rosińska,[138,52] M. P. Ross,[139] S. Rowan,[43] A. Rüdiger,[9] P. Ruggi,[27] K. Ryan,[44] S. Sachdev,[1] T. Sadecki,[44] L. Sadeghian,[24] M. Sakellariadou,[140] L. Salconi,[27] M. Saleem,[109] F. Salemi,[9] A. Samajdar,[134] L. Sammut,[126] L. M. Sampson,[94] E. J. Sanchez,[1] V. Sandberg,[44] B. Sandeen,[94] J. R. Sanders,[41] B. Sassolas,[23] B. S. Sathyaprakash,[82,95] P. R. Saulson,[41] O. Sauter,[113] R. L. Savage,[44] A. Sawadsky,[32] P. Schale,[67] J. Scheuer,[94] E. Schmidt,[33] J. Schmidt,[9] P. Schmidt,[1,61] R. Schnabel,[30] R. M. S. Schofield,[67] A. Schönbeck,[30] E. Schreiber,[9] D. Schuette,[9,32] B. W. Schulte,[9] B. F. Schutz,[95,9] S. G. Schwalbe,[33] J. Scott,[43] S. M. Scott,[22] E. Seidel,[11] D. Sellers,[6] A. S. Sengupta,[141] D. Sentenac,[27] V. Sequino,[29,17] A. Sergeev,[120] D. A. Shaddock,[22] T. J. Shaffer,[44] A. A. Shah,[128] M. S. Shahriar,[94] L. Shao,[34] B. Shapiro,[47] P. Shawhan,[72] A. Sheperd,[24] D. H. Shoemaker,[14] D. M. Shoemaker,[73] K. Siellez,[73] X. Siemens,[24] M. Sieniawska,[52] D. Sigg,[44] A. D. Silva,[15] A. Singer,[1] L. P. Singer,[76] A. Singh,[34,9,32] R. Singh,[2] A. Singhal,[16,31] A. M. Sintes,[96] B. J. J. Slagmolen,[22] B. Smith,[6] J. R. Smith,[26] R. J. E. Smith,[1] E. J. Son,[123] J. A. Sonnenberg,[24] B. Sorazu,[43] F. Sorrentino,[55] T. Souradeep,[18] A. P. Spencer,[43] A. K. Srivastava,[99] A. Staley,[46] M. Steinke,[9] J. Steinlechner,[43,30] S. Steinlechner,[30] D. Steinmeyer,[9,32] B. C. Stephens,[24] R. Stone,[97] K. A. Strain,[43] G. Stratta,[65,66] S. E. Strigin,[57] R. Sturani,[142] A. L. Stuver,[6] T. Z. Summerscales,[143] L. Sun,[131] S. Sunil,[99] P. J. Sutton,[95] B. L. Swinkels,[27] M. J. Szczepańczyk,[33] M. Tacca,[35] D. Talukder,[67] D. B. Tanner,[5] M. Tápai,[110] A. Taracchini,[34] J. A. Taylor,[128] R. Taylor,[1] T. Theeg,[9] E. G. Thomas,[53] M. Thomas,[6] P. Thomas,[44] K. A. Thorne,[6] K. S. Thorne,[59] E. Thrane,[126] S. Tiwari,[16,89] V. Tiwari,[95] K. V. Tokmakov,[117] K. Toland,[43] M. Tonelli,[20,21] Z. Tornasi,[43] C. I. Torrie,[1] D. Töyrä,[53] F. Travasso,[27,40] G. Traylor,[6] D. Trifirò,[10] J. Trinastic,[5] M. C. Tringali,[102,89] L. Trozzo,[144,21] K. W. Tsang,[13] M. Tse,[14] R. Tso,[1] D. Tuyenbayev,[97] K. Ueno,[24] D. Ugolini,[145] C. S. Unnikrishnan,[111] A. L. Urban,[1] S. A. Usman,[95] H. Vahlbruch,[32] G. Vajente,[1] G. Valdes,[97] M. Vallisneri,[59] N. van Bakel,[13] M. van Beuzekom,[13] J. F. J. van den Brand,[71,13] C. Van Den Broeck,[13] D. C. Vander-Hyde,[41] L. van der Schaaf,[13] J. V. van Heijningen,[13] A. A. van Veggel,[43] M. Vardaro,[49,50] V. Varma,[59] S. Vass,[1] M. Vasúth,[45] A. Vecchio,[53] G. Vedovato,[50] J. Veitch,[53] P. J. Veitch,[78] K. Venkateswara,[139] G. Venugopalan,[1] D. Verkindt,[7] F. Vetrano,[65,66] A. Viceré,[65,66] A. D. Viets,[24] S. Vinciguerra,[53] D. J. Vine,[58] J.-Y. Vinet,[62] S. Vitale,[14] T. Vo,[41] H. Vocca,[39,40] C. Vorvick,[44] D. V. Voss,[5] W. D. Vousden,[53] S. P. Vyatchanin,[57] A. R. Wade,[1] L. E. Wade,[81] M. Wade,[81] R. Walet,[13] M. Walker,[2] L. Wallace,[1] S. Walsh,[24] G. Wang,[16,66] H. Wang,[53] J. Z. Wang,[82] M. Wang,[53] Y.-F. Wang,[87] Y. Wang,[60] R. L. Ward,[22] J. Warner,[44] M. Was,[7] J. Watchi,[91] B. Weaver,[44] L.-W. Wei,[9,32] M. Weinert,[9] A. J. Weinstein,[1] R. Weiss,[14] L. Wen,[60] E. K. Wessel,[11] P. Weßels,[9] T. Westphal,[9] K. Wette,[9] J. T. Whelan,[115] B. F. Whiting,[5] C. Whittle,[126] D. Williams,[43] R. D. Williams,[1] A. R. Williamson,[115] J. L. Willis,[146] B. Willke,[32,9] M. H. Wimmer,[9,32] W. Winkler,[9] C. C. Wipf,[1] H. Wittel,[9,32] G. Woan,[43] J. Woehler,[9] J. Wofford,[115] K. W. K. Wong,[87] J. Worden,[44] J. L. Wright,[43] D. S. Wu,[9] G. Wu,[6] W. Yam,[14] H. Yamamoto,[1] C. C. Yancey,[72] M. J. Yap,[22] Hang Yu,[14] Haocun Yu,[14] M. Yvert,[7] A. Zadrożny,[124] M. Zanolin,[33] T. Zelenova,[27] J.-P. Zendri,[50] M. Zevin,[94] L. Zhang,[1] M. Zhang,[132] T. Zhang,[43] Y.-H. Zhang,[115] C. Zhao,[60] M. Zhou,[94] Z. Zhou,[94] S. J. Zhu,[34,9] X. J. Zhu,[60] M. E. Zucker,[1,14] and J. Zweizig[1]

(LIGO Scientific Collaboration and Virgo Collaboration)

S. Buchner[147,148], I. Cognard[149,150], A. Corongiu[151], P. C. C. Freire[152], L. Guillemot[149,150], G. B. Hobbs[153], M. Kerr[153], A. G. Lyne[154], A. Possenti[151], R. M. Shannon[153,155], B. W. Stappers[154], and P. Weltevrede[154]

[*]Deceased, March 2016. [♯]Deceased, March 2017. [†]Deceased, February 2017. [‡]Deceased, December 2016.

[1]*LIGO, California Institute of Technology, Pasadena, CA 91125, USA*
[2]*Louisiana State University, Baton Rouge, LA 70803, USA*
[3]*Università di Salerno, Fisciano, I-84084 Salerno, Italy*
[4]*INFN, Sezione di Napoli, Complesso Universitario di Monte S.Angelo, I-80126 Napoli, Italy*
[5]*University of Florida, Gainesville, FL 32611, USA*
[6]*LIGO Livingston Observatory, Livingston, LA 70754, USA*
[7]*Laboratoire d'Annecy-le-Vieux de Physique des Particules (LAPP), Université Savoie Mont Blanc, CNRS/IN2P3, F-74941 Annecy, France*

[8] *University of Sannio at Benevento, I-82100 Benevento, Italy and INFN, Sezione di Napoli, I-80100 Napoli, Italy*
[9] *Albert-Einstein-Institut, Max-Planck-Institut für Gravitationsphysik, D-30167 Hannover, Germany*
[10] *The University of Mississippi, University, MS 38677, USA*
[11] *NCSA, University of Illinois at Urbana-Champaign, Urbana, IL 61801, USA*
[12] *University of Cambridge, Cambridge CB2 1TN, United Kingdom*
[13] *Nikhef, Science Park, 1098 XG Amsterdam, The Netherlands*
[14] *LIGO, Massachusetts Institute of Technology, Cambridge, MA 02139, USA*
[15] *Instituto Nacional de Pesquisas Espaciais, 12227-010 São José dos Campos, São Paulo, Brazil*
[16] *Gran Sasso Science Institute (GSSI), I-67100 L'Aquila, Italy*
[17] *INFN, Sezione di Roma Tor Vergata, I-00133 Roma, Italy*
[18] *Inter-University Centre for Astronomy and Astrophysics, Pune 411007, India*
[19] *International Centre for Theoretical Sciences, Tata Institute of Fundamental Research, Bengaluru 560089, India*
[20] *Università di Pisa, I-56127 Pisa, Italy*
[21] *INFN, Sezione di Pisa, I-56127 Pisa, Italy*
[22] *OzGrav, Australian National University, Canberra, Australian Capital Territory 0200, Australia*
[23] *Laboratoire des Matériaux Avancés (LMA), CNRS/IN2P3, F-69622 Villeurbanne, France*
[24] *University of Wisconsin-Milwaukee, Milwaukee, WI 53201, USA*
[25] *LAL, Univ. Paris-Sud, CNRS/IN2P3, Université Paris-Saclay, F-91898 Orsay, France*
[26] *California State University Fullerton, Fullerton, CA 92831, USA*
[27] *European Gravitational Observatory (EGO), I-56021 Cascina, Pisa, Italy*
[28] *Chennai Mathematical Institute, Chennai 603103, India*
[29] *Università di Roma Tor Vergata, I-00133 Roma, Italy*
[30] *Universität Hamburg, D-22761 Hamburg, Germany*
[31] *INFN, Sezione di Roma, I-00185 Roma, Italy*
[32] *Leibniz Universität Hannover, D-30167 Hannover, Germany*
[33] *Embry-Riddle Aeronautical University, Prescott, AZ 86301, USA*
[34] *Albert-Einstein-Institut, Max-Planck-Institut für Gravitationsphysik, D-14476 Potsdam-Golm, Germany*
[35] *APC, AstroParticule et Cosmologie, Université Paris Diderot, CNRS/IN2P3, CEA/Irfu, Observatoire de Paris, Sorbonne Paris Cité, F-75205 Paris Cedex 13, France*
[36] *Korea Institute of Science and Technology Information, Daejeon 34141, Korea*
[37] *West Virginia University, Morgantown, WV 26506, USA*
[38] *Center for Gravitational Waves and Cosmology, West Virginia University, Morgantown, WV 26505, USA*
[39] *Università di Perugia, I-06123 Perugia, Italy*
[40] *INFN, Sezione di Perugia, I-06123 Perugia, Italy*
[41] *Syracuse University, Syracuse, NY 13244, USA*
[42] *University of Minnesota, Minneapolis, MN 55455, USA*
[43] *SUPA, University of Glasgow, Glasgow G12 8QQ, United Kingdom*
[44] *LIGO Hanford Observatory, Richland, WA 99352, USA*
[45] *Wigner RCP, RMKI, H-1121 Budapest, Konkoly Thege Miklós út 29-33, Hungary*
[46] *Columbia University, New York, NY 10027, USA*
[47] *Stanford University, Stanford, CA 94305, USA*
[48] *Università di Camerino, Dipartimento di Fisica, I-62032 Camerino, Italy*
[49] *Università di Padova, Dipartimento di Fisica e Astronomia, I-35131 Padova, Italy*
[50] *INFN, Sezione di Padova, I-35131 Padova, Italy*
[51] *MTA Eötvös University, "Lendulet" Astrophysics Research Group, Budapest 1117, Hungary*
[52] *Nicolaus Copernicus Astronomical Center, Polish Academy of Sciences, 00-716, Warsaw, Poland*
[53] *University of Birmingham, Birmingham B15 2TT, United Kingdom*
[54] *Università degli Studi di Genova, I-16146 Genova, Italy*
[55] *INFN, Sezione di Genova, I-16146 Genova, Italy*
[56] *RRCAT, Indore MP 452013, India*
[57] *Faculty of Physics, Lomonosov Moscow State University, Moscow 119991, Russia*
[58] *SUPA, University of the West of Scotland, Paisley PA1 2BE, United Kingdom*
[59] *Caltech CaRT, Pasadena, CA 91125, USA*
[60] *OzGrav, University of Western Australia, Crawley, Western Australia 6009, Australia*
[61] *Department of Astrophysics/IMAPP, Radboud University Nijmegen, P.O. Box 9010, 6500 GL Nijmegen, The Netherlands*
[62] *Artemis, Université Côte d'Azur, Observatoire Côte d'Azur, CNRS, CS 34229, F-06304 Nice Cedex 4, France*
[63] *Institut de Physique de Rennes, CNRS, Université de Rennes 1, F-35042 Rennes, France*
[64] *Washington State University, Pullman, WA 99164, USA*
[65] *Università degli Studi di Urbino 'Carlo Bo', I-61029 Urbino, Italy*

[66] *INFN, Sezione di Firenze, I-50019 Sesto Fiorentino, Firenze, Italy*
[67] *University of Oregon, Eugene, OR 97403, USA*
[68] *Laboratoire Kastler Brossel, UPMC-Sorbonne Universités, CNRS, ENS-PSL Research University, Collège de France, F-75005 Paris, France*
[69] *Carleton College, Northfield, MN 55057, USA*
[70] *Astronomical Observatory Warsaw University, 00-478 Warsaw, Poland*
[71] *VU University Amsterdam, 1081 HV Amsterdam, The Netherlands*
[72] *University of Maryland, College Park, MD 20742, USA*
[73] *Center for Relativistic Astrophysics and School of Physics, Georgia Institute of Technology, Atlanta, GA 30332, USA*
[74] *Université Claude Bernard Lyon 1, F-69622 Villeurbanne, France*
[75] *Università di Napoli 'Federico II', Complesso Universitario di Monte S.Angelo, I-80126 Napoli, Italy*
[76] *NASA Goddard Space Flight Center, Greenbelt, MD 20771, USA*
[77] *RESCEU, University of Tokyo, Tokyo, 113-0033, Japan.*
[78] *OzGrav, University of Adelaide, Adelaide, South Australia 5005, Australia*
[79] *Tsinghua University, Beijing 100084, China*
[80] *Texas Tech University, Lubbock, TX 79409, USA*
[81] *Kenyon College, Gambier, OH 43022, USA*
[82] *The Pennsylvania State University, University Park, PA 16802, USA*
[83] *National Tsing Hua University, Hsinchu City, 30013 Taiwan, Republic of China*
[84] *Charles Sturt University, Wagga Wagga, New South Wales 2678, Australia*
[85] *University of Chicago, Chicago, IL 60637, USA*
[86] *Pusan National University, Busan 46241, Korea*
[87] *The Chinese University of Hong Kong, Shatin, NT, Hong Kong*
[88] *INAF, Osservatorio Astronomico di Padova, Vicolo dell'Osservatorio 5, I-35122 Padova, Italy*
[89] *INFN, Trento Institute for Fundamental Physics and Applications, I-38123 Povo, Trento, Italy*
[90] *Università di Roma 'La Sapienza', I-00185 Roma, Italy*
[91] *Université Libre de Bruxelles, Brussels 1050, Belgium*
[92] *Sonoma State University, Rohnert Park, CA 94928, USA*
[93] *Montana State University, Bozeman, MT 59717, USA*
[94] *Center for Interdisciplinary Exploration & Research in Astrophysics (CIERA), Northwestern University, Evanston, IL 60208, USA*
[95] *Cardiff University, Cardiff CF24 3AA, United Kingdom*
[96] *Universitat de les Illes Balears, IAC3—IEEC, E-07122 Palma de Mallorca, Spain*
[97] *The University of Texas Rio Grande Valley, Brownsville, TX 78520, USA*
[98] *Bellevue College, Bellevue, WA 98007, USA*
[99] *Institute for Plasma Research, Bhat, Gandhinagar 382428, India*
[100] *The University of Sheffield, Sheffield S10 2TN, United Kingdom*
[101] *California State University, Los Angeles, 5151 State University Dr, Los Angeles, CA 90032, USA*
[102] *Università di Trento, Dipartimento di Fisica, I-38123 Povo, Trento, Italy*
[103] *Montclair State University, Montclair, NJ 07043, USA*
[104] *National Astronomical Observatory of Japan, 2-21-1 Osawa, Mitaka, Tokyo 181-8588, Japan*
[105] *Canadian Institute for Theoretical Astrophysics, University of Toronto, Toronto, Ontario M5S 3H8, Canada*
[106] *Whitman College, 345 Boyer Avenue, Walla Walla, WA 99362 USA*
[107] *School of Mathematics, University of Edinburgh, Edinburgh EH9 3FD, United Kingdom*
[108] *University and Institute of Advanced Research, Gandhinagar Gujarat 382007, India*
[109] *IISER-TVM, CET Campus, Trivandrum Kerala 695016, India*
[110] *University of Szeged, Dóm tér 9, Szeged 6720, Hungary*
[111] *Tata Institute of Fundamental Research, Mumbai 400005, India*
[112] *INAF, Osservatorio Astronomico di Capodimonte, I-80131, Napoli, Italy*
[113] *University of Michigan, Ann Arbor, MI 48109, USA*
[114] *American University, Washington, D.C. 20016, USA*
[115] *Rochester Institute of Technology, Rochester, NY 14623, USA*
[116] *University of Białystok, 15-424 Białystok, Poland*
[117] *SUPA, University of Strathclyde, Glasgow G1 1XQ, United Kingdom*
[118] *University of Southampton, Southampton SO17 1BJ, United Kingdom*
[119] *University of Washington Bothell, 18115 Campus Way NE, Bothell, WA 98011, USA*
[120] *Institute of Applied Physics, Nizhny Novgorod, 603950, Russia*
[121] *Seoul National University, Seoul 08826, Korea*
[122] *Inje University Gimhae, South Gyeongsang 50834, Korea*
[123] *National Institute for Mathematical Sciences, Daejeon 34047, Korea*
[124] *NCBJ, 05-400 Świerk-Otwock, Poland*
[125] *Institute of Mathematics, Polish Academy of Sciences, 00656 Warsaw, Poland*

[126] *OzGrav, School of Physics & Astronomy, Monash University, Clayton 3800, Victoria, Australia*
[127] *Hanyang University, Seoul 04763, Korea*
[128] *NASA Marshall Space Flight Center, Huntsville, AL 35811, USA*
[129] *ESPCI, CNRS, F-75005 Paris, France*
[130] *Southern University and A&M College, Baton Rouge, LA 70813, USA*
[131] *OzGrav, University of Melbourne, Parkville, Victoria 3010, Australia*
[132] *College of William and Mary, Williamsburg, VA 23187, USA*
[133] *Indian Institute of Technology Madras, Chennai 600036, India*
[134] *IISER-Kolkata, Mohanpur, West Bengal 741252, India*
[135] *Scuola Normale Superiore, Piazza dei Cavalieri 7, I-56126 Pisa, Italy*
[136] *Université de Lyon, F-69361 Lyon, France*
[137] *Hobart and William Smith Colleges, Geneva, NY 14456, USA*
[138] *Janusz Gil Institute of Astronomy, University of Zielona Góra, 65-265 Zielona Góra, Poland*
[139] *University of Washington, Seattle, WA 98195, USA*
[140] *King's College London, University of London, London WC2R 2LS, United Kingdom*
[141] *Indian Institute of Technology, Gandhinagar Ahmedabad Gujarat 382424, India*
[142] *International Institute of Physics, Universidade Federal do Rio Grande do Norte, Natal RN 59078-970, Brazil*
[143] *Andrews University, Berrien Springs, MI 49104, USA*
[144] *Università di Siena, I-53100 Siena, Italy*
[145] *Trinity University, San Antonio, TX 78212, USA*
[146] *Abilene Christian University, Abilene, TX 79699, USA*
[147] *Square Kilometer Array South Africa, The Park,*
Park Road, Pinelands, Cape Town 7405, South Africa
[148] *Hartebeesthoek Radio Astronomy Observatory, PO Box 443, Krugersdorp, 1740, South Africa*
[149] *Laboratoire de Physique et Chimie de l'Environnement et de l'Espace,*
LPC2E, CNRS-Université d'Orléans, F-45071 Orléans, France
[150] *Station de Radioastronomie de Nançay, Observatoire de Paris, CNRS/INSU, F-18330 Nançay, France*
[151] *INAF - Osservatorio Astronomico di Cagliari, via della Scienza 5, 09047 Selargius, Italy*
[152] *Max-Planck-Institut für Radioastronomie MPIfR, Auf dem Hügel 69, D-53121 Bonn, Germany*
[153] *CSIRO Astronomy and Space Science, Australia Telescope National Facility, Box 76 Epping, NSW, 1710, Australia*
[154] *Jodrell Bank Centre for Astrophysics, School of Physics and Astronomy,*
University of Manchester, Manchester M13 9PL, UK
[155] *International Centre for Radio Astronomy Research,*
Curtin University, Bentley, WA 6101, Australia
(Dated: 9/22/2017)